Impact of hypoxia on the expression of cell line markers and behavior of cultured glioma cell lines

LINA WIK LEISS

This thesis is submitted in partial fulfillment of the requirements for the degree of Master of Science

Department of Biomedicine

Faculty of Medicine and Dentistry

University of Bergen

Bergen, Norway

2011

Acknowledgements

The present work was carried out in the period August 2010 to June 2011 at the Department of Biomedicine, University of Bergen, Norway.

First of all, I would like to thank Per Øyvind Enger for being an excellent SUPERvisor! You have always been encouraging and optimistic, and your knowledge and enthusiasm has been truly inspiring for me. Even with a tightly packed schedule, you always found the time for helpful guidance throughout this period.

I would also like to thank my co-supervisor Linda Sleire. You have been an invaluable oracle in the lab, and I always met a smiling face when I came to your office with all my questions and concerns.

Great thanks to my research group, Oncomatrix Research Lab, for creating a friendly and supportive atmosphere. Especially thanks to Tao for teaching me western blotting and to Ercan for teaching me pcr and for enormous help towards the completion of this thesis. Also thanks to Agnete, who helped me with the flow cytometry.

To my parents; thank you for putting me up and influencing me (genetically and environmentally) to choose this path, and for always believing in me although not fully understanding what my education and daily life aims at.

Finally, to all my fellow students – the last two years have been GREAT!

Lina Leiss
May 2011

Summary

Glioblastoma multiforme (GBM) constitute over 50 % of primary brain tumors in adults. The tumor is heterogeneous and highly infiltrative. Its nature makes it extremely aggressive and incurable. Thus, today's treatment modalities only have a palliative function and provide a modest survival benefit. This states the need for further research to reveal the biological mechanisms behind GBM development.

The name glioblastoma *multiforme* reflects the expression of markers of many different CNS cell lineages in this tumor. Notably, GBMs have been reported to comprise cells that express stem cell markers, and it is postulated that glioma stem cells is the cell type initiating and maintaining this tumor. Also, several lines of evidence strongly suggest that hypoxia is a cancer stem cell niche. Furthermore, hypoxia is associated with poor prognosis in many solid cancers, being implicated in induction of radio- and chemoresistance and in tumor invasion. Hence, hypoxia and cancer stem cells may be two factors that contribute to the failure to treat this tumor. They might therefore be candidates which can be targeted in new therapeutical strategies for GBM.

To assess the expression of cancer stem cell markers in hypoxia, five glioma cell lines were cultured for various time periods in normoxic (21 %) and hypoxic (0.5 and 2 %) conditions. Expression of a panel of cell lineage markers was investigated in the different oxygen conditions. Additionally, cell behavior in hypoxia compared to normoxia was evaluated by investigating proliferation, migration and apoptosis.

We found that none of the stem cell markers that we looked at were upregulated in hypoxia, which is contradictory to previous reports. Instead, these stem cell markers and the astrocytic marker GFAP were all downregulated. Furthermore, cell proliferation and migration both decreased in hypoxia. This points at an overall slow down of the glioma cell machinery in hypoxia.

Other studies have mainly been performed on small selections of biopsy material cultured in serum free medium, and this approach should be included in the present study in the future.

Abbreviations

AML	Acute myeloid leukemia
ARF ($p14^{ARF}$)	Alternate reading frame
ARNT	Aryl hydrocarbon receptor nuclear translocator
bev	Bevacizumab
bHLH	basic Helix-Loop-Helix
BrdU	Bromodeoxyuridine
BSA	Bovine serum albumin
CBP	CREB binding protein
CNS	Central nervous system
CREB	cAMP response element binding
CSC	Cancer stem cell
C-TAD	C-terminal transactivation domain
DMEM	Dulbecco's Modified Eagle's Medium
DMSO	Dimethyl Sulfoxide
ECIS	Electric cell-substrate impedance sensing
EDTA	Ethylenediaminetetraacetic acid
EGFR	Epidermal growth factor receptor
EPO	Erythropoietin
EtBr	Ethidium bromide
FCM	Flow cytometry
FDA	(US) Food and Drug Administration
FIH	Factor inhibiting HIF
FITC	Fluorescein Isothiocyanate
GAPDH	Glyceraldehyde-3-phosphate dehydrogenase
GBM	Glioblastoma multiforme
GLUT1	Glucose transporter 1
Gy	Gray
HIF	Hypoxia inducible factor
HRE	Hypoxia response element
HRP	Horseradish peroxidase
ICC	Immunocytochemistry
INK4a ($p16^{INK4a}$)	Inhibitor of kinase 4a (also CDKN2A)
LOH	Loss of heterozygosity
MDR1	Multi drug resistance gene 1
MMP-2	Matrix metalloproteinase 2
mTOR	Mammalian target of rapamycin
NLS	Nuclear localization signal
N-TAD	N-terminal transactivation domain
Oct-4	Octamer binding transcription factor 4
ODDD	Oxygen dependent degradation domain
PAI-1	Plasminogen activator inhibitor-1
PAS	Per-Arnt-Sim
PFA	Paraformaldehyde
PFK	Phosphofructokinase
PHD	Prolyl hydroxylase
PI	Propidium Iodide
PI(3)K	Phosphatidylinositol 3-kinase
PS	Phosphatidyl serine

PTEN	Phosphatase and tensin homologue
qRT-PCR	Quantitative reverse transcriptase polymerase chain reaction
RAS	Rat sarcoma
RB	Retinoblastoma
ROS	Reactive oxygen species
RTK	Receptor tyrosine kinase
TF	Tissue factor
TMZ	Temozolomide
TP53	Tumor protein 53
tPA	tissue plasminogen activator
VEGF	Vascular endothelial growth factor
VHL	von Hippel-Lindau
WB	Western blotting
WHO	World Health Organization

Table of contents

1 Introduction

1.1 Cancer

Caused by successive malignant changes – mutations – in the DNA of one cell, cancer is a disease of the genome rather than of an organ. Still, the disease manifests as an abnormal proliferating mass in the body part where the transformed cell originates. The cancer cells acquire the abilities to invade surrounding tissue, metastasize and eventually kill the patient as an extensive disease affecting multiple organs. Research over the last decades has advanced our understanding of many aspects of cancer, and dramatically improved the prognosis for some cancer types. However, basic mechanisms mediating tumor initiation and progression are still incompletely understood. Thus, despite immense amounts of money and man hours spent on research the last decades, cancer still stands out as a major cause of death and morbidity, causing approximately 13% of all deaths[1] globally.

1.1.1 Cancer development

A review published in *Cell* by Hanahan and Weinberg (2000) sums up the current understanding of cancer. Hanahan and Weinberg introduced the well known concept *The Six Hallmarks of Cancer*. The hallmarks can be explained as a set of abilities that a cell must acquire in order to transform into a malignant cancer cell: the cell has gained the ability of unlimited division; it has become insensitive to anti-growth factors; it is self-sufficient in growth signals; it is resistant to apoptotic signals; it can promote angiogenesis and it can invade other tissues and metastasize[2]. Over the past decade the understanding of tumor biology has evolved, which has revealed the need of further cancer hallmarks. Recently, Hanahan and Weinberg published an updated version of their Hallmarks[3]. Emphasized is the cancer cell's capability to manipulate its stroma to create an advantageous microenvironment. Two enabling characteristics have been added; a prerequisite for evolution of the hallmarks, namely genomic instability, and tumor promoting inflammation. Additionally, a pair of new hallmarks have been suggested, the ability to avoid immune destruction and to deregulate metabolism in order to sustain continued growth[3].

Cancer is caused by abnormal changes in the DNA, and several changes are required for transformation of a normal cell into a cancer cell. Thus, cancer cells acquire several different

mutations, and cells that harbor mutations which confer a growth advantage are selected. This way, tumors evolve in a clonal manner arising from a single mutated cell[4]. Although, the very first genetic lesions that lead to development of a tumor may be inherited, most people that are diagnosed with cancer accumulate the mutations throughout their lives. Mutations may arise spontaneously or may be caused by environmental factors. In either case they may arise in what is called tumor suppressor genes and oncogenes. Oncogenes are genes that encode proteins that promote cell growth and division. Mutations cause an oncogene to be overexpressed or their gene products are rendered overactive. The gene may for example encode a growth factor or a component within a mitotic signaling cascade inside the cell. With overexpression or over-activity of the protein, the mutated gene promotes cell growth and division stronger than normal[5]. Oncogenic mutations are dominant, which means that only one allele needs to become mutated in order to influence cancer develoment[5]. Tumor suppressor genes on the other hand encode proteins that inhibit cell cycle progression, or they encode proteins promoting apoptosis in case of deleterious stress to the cell[5]. A well known tumor suppressor is p53, which is mutated in over 50 % of all cancers. p53 induces apoptosis in case of irreparably damaged DNA[6]. Both alleles of a tumor suppressor gene have to become mutated in order to influence cancer development, hence mutations in tumor suppressor genes are recessive mutations[5]. There are two main consequences of activated oncogenes or inactivated tumor suppressor genes; first, the proofreading machinery that normally prevents a damaged cell from dividing is not working and the signaling pathways mediating programmed cell death are disrupted. Secondly, the cell achieves stronger mitotic signals and divides faster than normal. This leads to increasing genomic instability, additional mutations and uncontrolled development of an abnormal cell mass.

All cells must be in vicinity to blood vessels in order to both receive nutrients, growth factors and oxygen, and to dispose waste products from their metabolism. This applies for tumor cells as well. When the tumor reaches a certain size, the increasing cell mass outgrows its blood vessel supply[7]. As a survival response tumor cells promote angiogenesis, the sprouting of new blood vessels from existing ones. This is mediated by secretion of vascular endothelial growth factor (VEGF) that is the major inducer of angiogenesis. VEGF is upregulated in response to both hypoxia and different growth factors[8]. VEGF induces destabilization of existing vessels, proliferation, migration and survival of endothelial cells that subsequently form new blood vessels[5, 8]. Cancer cells also release various other signaling molecules with a broad range of biological effects on the microenvironment, including remodeling of the extracellular matrix

and the tumor vasculature[5]. Since tumor cells almost exclusively escape their primary site through the blood or lymphatic system, angiogenesis is a key event in cancer cell metastasis. Since most cancer related deaths result from metastasis, angiogenesis is also coupled to overall tumor aggressiveness[9]. The metastatic process starts with migration of cancer cells from the primary site to a blood vessel, where the cells intravasate into the blood circulation. Cells are transported with the blood flow and eventually they get trapped in another body part, either by size restriction or by specific interactions[9]. Here, cells may extravasate and colonize surrounding tissue to form a secondary tumor, a metastasis[5, 9]. The whole process depends on a range of factors, including the ability to evade immune destruction, altered expression of cell adhesion molecules, as well as activation of enzymes that break down the extracellular constituents that restrain cells to one place[9]. Moreover, when the metastasizing cancer cells reach their final destination, the microenvironment must be permissive to sustain growth of the cancer cells. As reviewed by Ribatti *et al,* this is known as the "seed and soil theory" already proposed by Stephen Paget in 1889, and explains why certain cancers tend to spread to specific organs[10].

1.2 Brain Cancer

Cancers of the central nervous system (CNS) are classified according to their resemblance with the main cell types of the CNS. Thus, gliomas are similar to glial cells of the brain and can be subdivided into oligodendrogliomas, ependymomas and astrocytomas[11]. Astrocytomas are the most common brain cancers, and together with other CNS tumors, astrocytomas are given WHO grades I-IV corresponding to malignancy. This grading is based on histological criteria such as mitotic activity, anaplasia, nuclear atypia, microvascular proliferation and presence of pseudopalisading necrosis[11]. Tumor grade correlates with prognostic outcome, and provides the basis for deciding treatment regimen[11].

1.2.1 Glioblastoma multiforme

Each year about 19,000 persons are diagnosed with malignant primary brain tumor in the United States[12]. Of these, Glioblastoma multiforme (GBM) constitutes over 50 % of the cases, which makes it the most common primary brain tumor. Radical surgery is impossible due to its highly infiltrative growth and radio- and chemotherapy have a limited effect. Thus, the

prognosis for GBM patients is extremely poor, with a median survival time of about 14 months[13], and almost 100 % mortality rates.

Ionizing radiation is the only established risk factor for primary brain tumors. In addition Li-Fraumeni syndrome, Turcot syndrome, tuberous sclerosis and neurofibromatosis are associated with an increased risk of developing GBM as well as other cancer types[14]. Epidemiological data also suggest that there exists a non-syndromal genetic predisposition to GBM, but the genetic basis for this is not known[14]. As such, people of Caucasian origin are diagnosed more often with GBM. Also, men have a higher prevalence than women (3:1), and the incidence rate increases with age. Still, the possible risk factors account for a small part of the cases only (reviewed in[15]).

Table 1.2.1: Astrocytic tumors graded according to the WHO system described above[11].

Astrocytic tumor	Grading	Criteria
Pilocytic Astrocytoma	I	Low proliferative potential, possible curable by surgical resection only.
Diffuse Astrocytoma	II	Infiltrative, low level of proliferation, nuclear atypia. Tend to recur as higher grade glioma.
Anaplastic Astrocytoma	III	Infiltrative, mitotic activity, nuclear atypia, anaplasia.
Glioblastoma Multiforme	IV	Highly infiltrative, and in addition to grade III criteria: microvascular proliferation, necrotic areas, pseudopalisades.

1.2.2 Mutations in GBM

Although there is no unifying genetic signature common to all GBMs, they are still characterized by certain patterns of mutations which are present in varying proportions of GBMs. *The Cancer Genome Atlas Research Network* has combined data from a multi-domain analysis of 206 glioblastomas. Their compilation of data on copy number alterations, abundance of coding genes and non-coding microRNAs and single nucleotide polymorphisms has revealed three signaling networks that are frequently altered in GBMs: the RTK/RAS/PI(3)K (88%), p53 (87%) and RB (78%) pathways[16].

GBM can arise *de novo* or as a malignant progression from lower grade astrocytic tumors[17]. These are called primary and secondary GBM, respectively. Primary GBM is the most frequent variant and is more common among elderly GBM-patients. Secondary GBM occurs more often in younger patients[17]. Even though the two GBM variants have the same histological appearance, the chromosomal aberrations that characterize the two types of GBM are somewhat different (reviewed in[18]), as listed in table 1.2.2.

Table 1.2.2: Characteristic chromosomal aberrations found in primary and secondary GBMs. The percentage of GBMs harboring each mutation is indicated in brackets. Adapted from Ohgaki and Kleihues[18].

Astrocytic tumor	Astrocyte or precursor stem cell	
	Development of primary GBM	**Development of secondary GBM**
Low grade astrocytoma (grade II)	no clinical manifestation	TP53 mutation (59%)
Anaplastic astrocytoma (grade III)	no clinical manifestation	TP53 mutation (53%)
GBM (grade IV)	RB methylation (14%) LOH 22q (41%) LOH 19q (6%) LOH 10q (70%) LOH 10p (47%) EGFR amplification (40%) EGFR overexpression (60%) P16INK4a deletion (31%) p14^{ARF} (76%) TP53 mutation (28%) PTEN mutation (25%)	RB methylation (43%) LOH 22q (82%) LOH 19q (54%) LOH 10q (63%) LOH 10p (8%) EGFR amplification (8%) EGFR overexpression (10%) P16INK4a deletion (19%) p14^{ARF} (76%) TP53 mutation (65%) PTEN mutation (4%)

1.3 Hypoxia

Hypo- is a prefix from the Ancient Greek language and means under, while -oxia comes from oxygen, hence hypoxia means low oxygen. The physiological oxygen concentration in adults varies with tissue and even in regions of the same organ[19], but the average body oxygen concentration is around 3 %[20]. Oxygen levels below the physiological concentration are considered being hypoxic, and brain tumor hypoxia is defined to be between 0.1 and 2.5 %[21]. Hypoxia triggers necessary physiological responses such as wound healing. Several pathological conditions may lead to tissue hypoxia, for example embolism, thrombosis, environmental factors and tumor growth[22]. Hypoxia has a profound effect on all oxygen utilizing cells, and processes such as apoptosis, cell signaling, metabolism and cell cycle progression are all regulated in response to hypoxia[23]. In response to a hypoxic state, cells can be damaged and die, or they may adapt to scarcer conditions[24].

Although several isoforms have been found[25], the most studied transcription factor responsible for an hypoxic response is hypoxia inducible factor 1 (HIF-1)[23]. HIF-1 is a heterodimer consisting of two basic helix-loop-helix (bHLH)/PAS (Per Arnt Sim) monomers named HIF-1α and ARNT (aryl hydrocarbon receptor nuclear translocator)[26]. ARNT is also known as HIF-1β[26, 27].
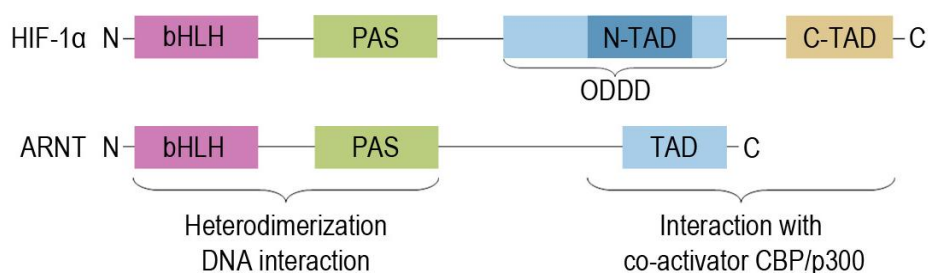
Figure 1.3.1: Schematic overview of HIF-1α and ARNT monomers. bHLH/PAS domains constitute the dimerization surface where the monomers contact each other. bHLHs also make up the DNA-binding structures of HIF. ODDDs (oxygen dependent degradation domains) are targeted by prolyl hydroxylase. N-TADs and C-TADs (transcriptional-activation domains) interact with transcriptional co-activators, and C-TAD is also negatively regulated by hydroxylation. Adapted from Brahimi-Horn and Pouyssegur[25].

Table 1.3.1: bHLH/PAS proteins and isoforms involved in the hypoxic response

Protein	Function
HIF-1α	Both are activated in response to hypoxia, but have different target genes[25]
HIF-2α	
HIF-3α	Negative regulator of HIF-1α and HIF-2α[25]
ARNT (HIF-1β)	Not oxygen-regulated, dimerizes with HIF-1 and -2α subunits (and other nuclear receptors[28]) to form the active transcription factor
ARNT2 (HIF-2β)	Less investigated, exact function not known[28]
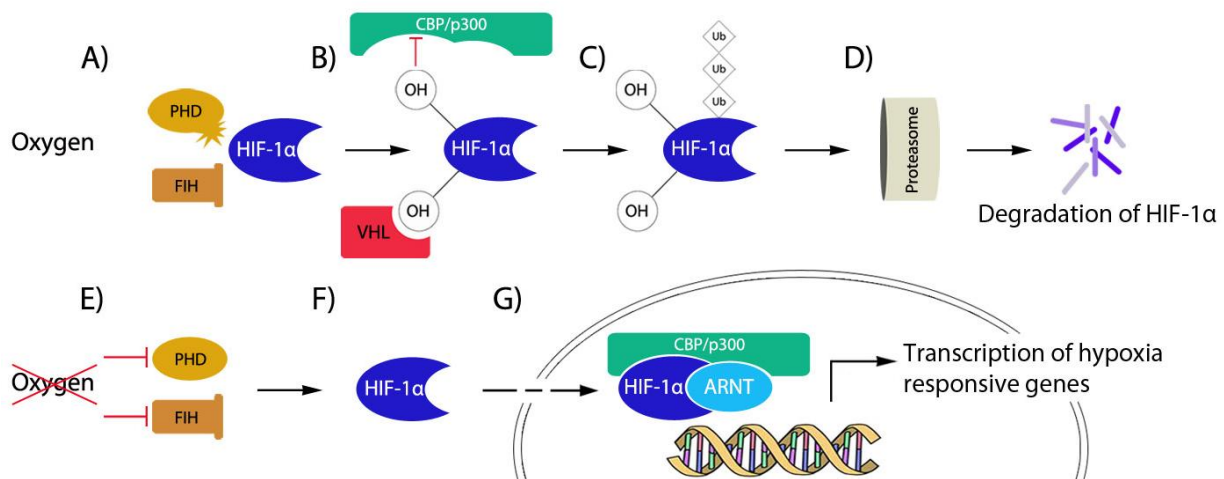
Figure 1.3.2: (A) When physiological oxygen levels are present, prolyl hydroxylation and asparginyl hydroxylation of HIF-1α is catalyzed by prolyl 4-hydroxylase (PHD) and factor inhibiting HIF (FIH). (B) Asparginyl hydroxylation inhibits HIF-1α from interaction with the transcriptional co-activators CBP and p300. Prolyl hydroxylation allows the von Hippel-Lindau tumor suppressor (VHL), an E3-ligase, to interact with and poly-ubiquitinate HIF-1α. (C) Ubiquitination targets HIF-1α for degradation in the proteasomal pathway (D). (E) When oxygen is not available, PHD and FIH are inhibited, thus HIF-1α is stabilized (F) and translocates to the nucleus. (G) Here, HIF-1α heterodimerizes with ARNT. HIF-1 is now a functional transcription factor that binds to HREs and activates transcription[25].

Under normoxic conditions, the constitutively expressed HIF-1α is located in the cytoplasm. Here, HIF-1α is continuously degraded through the proteasomal pathway (Shown in figure 1.3.2 A-D). In lack of oxygen, unhydroxylated HIF-1α reveals its nuclear localization signal (NLS) and is translocated to the nucleus where it heterodimerizes with ARNT[23]. HIF-1 targets promoters with the sequence 5' – RCGTG – 3' (R=A/G), which is called the hypoxia responsive element (HRE)[25, 27]. As reviewed by Semenza (2003), more than 60 genes

involved in such various functions as cell proliferation, motility, apoptosis, morphology and metabolism are found to be regulated in response to hypoxia[29]. Furthermore Iyer *et al* demonstrated that in mice, HIF-1α $^{-/-}$ embryos died within embryonic day 10.5[30]. This underscores the extensive importance of this transcription factor in development and throughout life.

Table 1.3.2 A selection of proteins encoded by hypoxia-activated genes (modified from Fandrey[31]).

Protein	Function
Erythropoietin (EPO)	Increases production of red blood cells in the bone marrow[31, 32]
Glucose transporter 1 (GLUT1)	Transports glucose into the cell[31, 33]
Phosphofructokinase (PFK)	Key regulator in the glycolytic pathway, (phosphorylates glucose-6-phosphate)[31, 34]
Enolase	Glycolytic enzyme (2-phosphoglycerate to phosphoenolpyruvate)[31, 34]
Vascular endothelial growth factor (VEGF)	Stimulates vasculogenesis and angiogenesis[31, 35]

1.3.1 The role of hypoxia in cancer

When tumors grow beyond 1-2 mm in diameter, they outgrow the distance by which oxygen can diffuse into the tumor center from nearby vessels[36]. In addition, tumor neovasculature is highly aberrant and inefficient in delivering oxygen and nutrients to surrounding cells[37]. Hence, the core of the tumor mass will become hypoxic. This can lead to apoptosis and necrosis, as some tumor cells lack the ability to adapt to the harsher conditions of the hypoxic area. A portion of cells may have acquired mutations in pro-apoptotic genes such as p53, which favor their survival despite hypoxic environments[24, 38]. Tumor cells upregulate genes associated with survival programs. For instance, VEGF is secreted and the number of glycolytic enzymes are increased (reviewed by Fandrey[31]). The master regulator responsible for these compensatory gene expression changes is HIF-1[23, 39].

Tumor hypoxia has long been recognized as a poor prognostic factor, and already more than half a century ago physicist Louis Harold Gray suggested that there was a connection between tissue oxygen concentration and response to irradiation[40]. Radiation creates reactive oxygen

species (ROS) through two mechanisms; either by radiolysis of water molecules which again react with DNA, or by directly ionizing DNA. In both instances, a free radical is created in the DNA molecule[5]. In an oxygenated tumor the radical can react further with O_2 and give a fixed damage in the cell's DNA (figure 1.3.1.1). Radiation induced damage is therefore dependent on the presence of oxygen in the tissue. In hypoxic areas of a tumor, free radicals will not be created in sufficient amounts for radiation therapy to be fully effective. Notably, the direct ionization of DNA is reversible in lack of oxygen[41].
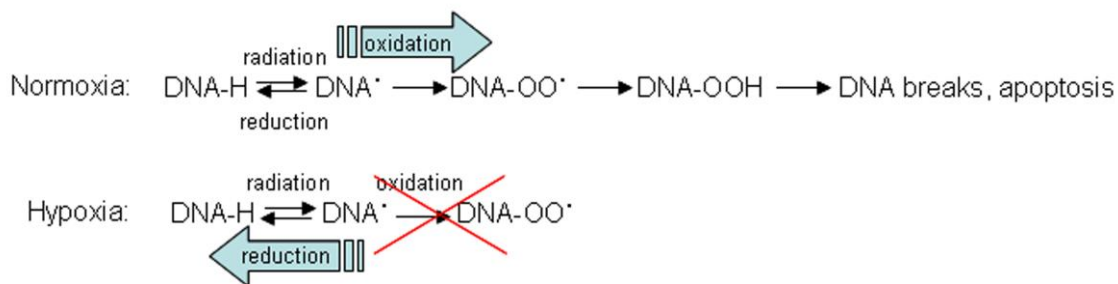
Figure 1.3.1.1: Direct action of irradiation on DNA. In presence of oxygen the reaction proceeds through oxidation to the more stable forms DNA-OO· and DNA-OOH, which causes permanent damage to DNA and induces cell death. In absence of oxygen, the first step where DNA· is formed is reversible, and there is no permanent change to DNA. A blue arrow indicates the favored reaction in each condition. Modified from De Ridder *et al*[41].

Furthermore, cancer cells have other strategies to protect themselves against ROS-induced cell death. As mentioned above, rising HIF-1α levels induce genes which enable the cells to cope with lower oxygen and nutrient levels[31]. In addition, since hypoxia acts as a selection pressure for cells resistant to apoptosis, the cells that are selected will also be resistant to radiotherapy that induces apoptosis by causing DNA damage[24, 36, 38]. In healthy cells, damage from ROS-production causes cell cycle arrest and DNA repair if the lesion is mild. In case of irreparable damage, the p53 pathway induces apoptosis[42]. In tumor cells however, loss of cell cycle control and disruption of apoptotic pathways allow for progression through the cell cycle, even in the presence of extensive DNA changes[38].

Additionally, tumor cells display increased levels of antioxidant production, which represents an additional defense mechanism against ROS. High levels of antioxidants will quench ROS before they are allowed to react with the DNA, causing further damage[43]. As previously reported by Schwartz *et al.,* hypoxia may also mediate resistance to irradiation by another more indirect mechanism. Even though an area is not hypoxic at the time radiation is given, it

may become hypoxic in response to radiation. After radiation treatment, tumor vasculature function is disrupted; hence the irradiated area develops hypoxia. HIF-1 induced transcription follows, and may play a role in helping tumor cells survive damage to the microenvironment caused by radiation[44].

The hypoxic selection of cells resistant to apoptosis also mediates resistance to chemotherapy. Moreover, hypoxia has been shown to upregulate expression of the multidrug resistance ABC-transporter P-glycoprotein (MDR1)[45]. This transmembrane channel transports different xenobiotics out of the cell, including chemotherapeutic drugs[46]. Moreover, Brown *et al* emphasized the significance of the longer distance between blood vessels and hypoxic cells compared to normoxic cells. Due to this difference hypoxic cells may be less exposed to intravenously administered cytotoxic agents than normoxic cells. In addition, hypoxic cells tend to divide slower, and they are therefore less influenced by chemotherapy, which principally act on rapidly dividing cells[36].

Probably, none of these factors alone can explain resistance to apoptosis inducing therapies such as radiation. Most likely a hypoxic environment that selects for apoptosis resistant cancer cells combined with the versatile ability to withstand ROS effects on DNA enables cancer cells to survive radiation therapy.

1.3.2 Hypoxia in brain tumors is associated with a more aggressive phenotype

Glioblastoma Multiforme is characterized by florid angiogenesis and highly infiltrative growth. As reviewed by Rong *et al* (2006), the characteristics that distinguish high grade from low grade gliomas are the presence of pseudopalisading necrotic foci and microvascular hyperplasia[47]. Necrotic areas are anoxic, and palisading cells at the rim of these necrotic foci will receive slightly more oxygen and become hypoxic. The consequence is VEGF upregulation and hypoxia-driven angiogenesis in proximity to necrotic areas[47]. Thus, hypoxia and angiogenesis are key events in brain tumor progression.

Notably, several lines of evidence strongly suggest that hypoxia promotes invasive growth as well. Histological examinations reveal that cells in the palisading region are migrating outwards and away from the necrotic region[47, 48]. Also, matrix metalloproteinase-2 (MMP-2)

is found to be upregulated, which is associated with migratory behavior[48, 49]. Pennacchietti *et al* also reported that c-Met tyrosine kinase, a high affinity receptor for the pro-invasive cytokine HGF, is induced by hypoxia and is upregulated in hypoxic areas of human tumors[50]. Furthermore they demonstrated that hypoxia amplified hepatocyte growth factor (HGF) signaling and increased tumor invasion. Hypoxia therefore seems to induce migratory properties in astrocytoma cells, which may account for the ability of GBM to expand and spread throughout the brain so rapidly[47]. Thus, both angiogenesis and glioma cell invasion, which contribute to the aggressive phenotype of brain tumors, are regulated by hypoxia.
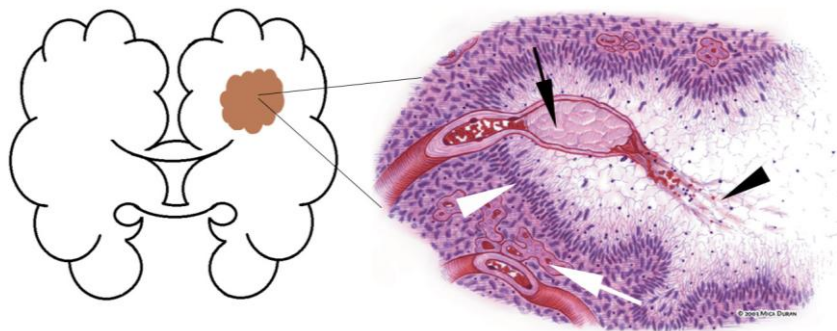
Figure 1.3.2: Schematic drawing of pseudopalisading necrosis. Central in the tumor lays foci of necrotic cells around a regressing vessel (black arrowhead). The vessel is obstructed by a clot (black arrow). Surrounding, hypoxic cells are migrating away from the central necrosis, causing a rim of denser cell layers that resemble palisading tissue, wherefrom the name pseudopalisading comes (white arrowhead). Microvascular proliferation (white arrow) is induced by VEGF-secreting hypoxic cells. Adapted from[51](review).

As previously mentioned, the traditional view is that expanding tumors outgrow their vascular supply and that hypoxia and tumor necroses arise in cells furthest from the vasculature. Another theory applicable to GBMs is that the regression of clotted and necrotic vessels caused by thrombosis leads to necrotic regions with outwardly migrating cells[52]. This is supported by the fact that thrombosed vessels are found in virtually all GBMs[48]. An important factor contributing to thrombosis in GBMs is the tissue factor (TF)[52]. TF is normally expressed in perivascular cells, and exists both as a transmembrane receptor and in a soluble form. TF is activated when contacting its ligand, which is only present in blood plasma. Through a series of events this receptor-ligand complex leads to formation of a blood clot[52]. With the aberrant and leaky vasculature of a tumor, TF will easily bind its ligand and lead to

thrombosis. The TF-gene is controlled by several hypoxia driven promoters, which further states the role of TF mediated thrombosis and in GBM hypoxia and necrosis[47, 53]. Moreover, the strongly expressed VEGF cause upregulation of both tissue plasminogen activator (tPA) and its inhibitor plasminogen activator inhibitor (PAI-1). By generating plasmin, tPA normally breaks down blood clots. PAI-1 is inhibiting this action, which results in lower fibrinolytic activity, further contributing to the prothrombotic status of GBM patients[54].

1.3.3 Hypoxia, cancer and cancer stem cells

As reviewed by Reya *et al* stem cells are defined as cells that have the ability of infinite self-renewal, giving rise to identical cells that maintain their undifferentiated state (symmetrical division). At the same time, they are multipotent and capable of giving rise to the specialized cells that make up and organ (asymmetrical division)[55]. Both stem cells and cancer cells have the ability of indefinite division, which gave rise to the theory that there is a "cancer stem cell" (CSC) responsible for the formation and growth of tumors[55]. The bulk of evidence for existing CSCs are found in acute myeloid leukemia[55], and a debate has been going on for many years whether CSCs or stem like cells exist for solid tumors. On one side is the hypothesis that essentially all cells of the heterogeneous tumor have the same ability of unlimited self-renewal and contribute equally to tumor growth and progression[56]. On the other side is the theory which implies that a small population of CSCs sustains the tumor by undergoing asymmetric division. In brain tumors, these cells may arise from transformed neural stem cells, or by dedifferentiation of transformed mature cells. Independent of which cell type they arise from, undergoing asymmetrical division is thought to preserve their stem like character while populating the tumor with more differentiated cells with limited proliferative potential[55]. Importantly the current treatment failures for many cancer types, including GBMs, have been attributed to the presence of CSCs. Based on the increased ability of normal stem cells to resist chemotherapy, these CSCs may be implicated in drug resistance[57, 58]. Thus, cancer drugs will have to target CSCs specifically, and not only their more differentiated progeny. Otherwise CSCs will re-populate the tumor after the treatment is stopped[9].
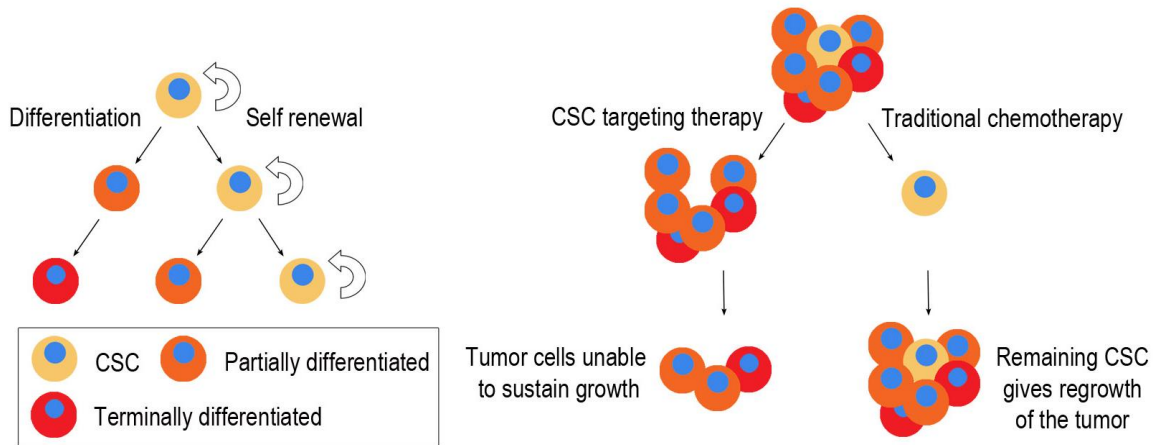
Figure 1.3.3: The cancer stem cell hypothesis and its therapeutic implications. Tumors are hierarchically organized: CSCs have the ability to self-renew as well as reconstitute all the different tumor cell types through differentiation (left panel). If the CSC pool is successfully eradicated through targeted therapies, the remaining cells will be unable to cause a tumor relapse. However, incomplete depletion of the CSC pool will inevitably be followed by tumor recurrence due to CSC self-renewal (right panel).

Hypoxia preserves the dedifferentiated state of normal neural stem cells and influences cell fate, while 20 % oxygen promotes differentiation[59, 60]. Thus hypoxia may play a similar role in solid tumors, by creating a niche for CSCs in which they are maintained in an undifferentiated state. Several groups have reported an increased fraction of cells expressing stem cell markers such as CD133 (Prominin-1) when different brain tumor cells are cultured in hypoxia[61-63]. Furthermore, co-expression of HIF-2α and CD133 has been reported[61], implicating HIF-2α as a transcription factor mediating survival, self-renewal and stemness in a hypoxic environment. Among transcriptional targets of HIF-2α are the genes OCT4 and SERPINB9[64]. The Oct-4 protein is itself a transcription factor and is associated with self-renewal[64]. SerpinB9 is a protease inhibitor linked to mediating immune evasion of CSCs[65]. In addition, HIF-2α seems to be active in glioma stem cells but not in "normal" glioma cells or brain progenitor cells[61, 66], suggesting that HIF-2α is regulating gene expression specifically in glioma stem cells. Overexpression of HIF-1α did not increase expression of typical stem cell markers, while overexpression of HIF-2α resulted in upregulation of stem cell markers such as CD133, Oct-4, and a component of the Notch pathway, MAML3 (Seidel *et al*). Moreover, Li *et al* performed immunohistochemistry on glioblastoma biopsy specimens and showed expression of HIF-2α and CD133 in a few cells around necrotic areas, while the majority of tumor cells expressed HIF-1α[61], suggesting that HIF-2α is a marker of glioma stem cells.

Together, these findings establish hypoxic areas within tumors as the microenvironmental niche that sustains CSCs. Since HIF-2α expression is restricted to the subpopulation of glioma stem cells it may provide a target by which therapy can be directed against the tumor initiating cells[61].

1.4 Therapy

1.4.1 Conventional therapies for Glioblastoma Multiforme

Although there is a multimodal treatment regiment in use for GBM patients, it is mainly palliative and provide only modest survival benefit[67]. This is due to the highly infiltrative nature of the tumor, which makes radical surgery impossible[67]. Symptoms are mainly caused by intracranial pressure due to the mass effect of the tumor and the surrounding edema or by destruction of functional brain tissue due to tumor invasion. Symptoms of increased intracranial pressure include headaches, nausea and drowsiness, while tumor invasion may cause personality changes, paresis and epileptic seizures, depending on the location. Therefore, corticosteroids and antiepileptic drugs are often administered until surgery has been performed[68]. In addition to surgery, radiation therapy (total dose 60-65 Gy) with concomitant and adjuvant chemotherapy is routinely given, as Stupp *et al* (2005) reported that a combination of radio- and chemotherapy with the alkylating agent Temozolomide (TMZ) increases overall survival with approximately two and a half months[13, 68] compared to radiotherapy alone.

1.4.2 New approaches to treatment

A huge number of clinical trials for testing drugs that potentially act against GBM are currently ongoing. Some compounds that target deregulated pathways have been FDA-approved for treatment of GBM as well. Since GBMs are highly vascular tumors, they may be attractive candidates for anti-angiogenic therapies. The VEGF inhibitor Bevacizumab/Avastin (bev) was FDA-approved for GBM treatment in 2009[69]. Bev is a recombinant humanized antibody directed against secreted VEGF, hence bev targets angiogenesis indirectly. However, despite a high initial response rate to bev, there seems to be no overall improved

survival, and even a rapid clinical decline after treatment has been terminated[70]. Notably, bev has been associated with increased invasion[71].

Epidermal growth factor receptor (EGFR) activity or abundance is commonly altered in GBMs, and small molecules and antibodies targeting the EGF-receptor have been extensively studied. Erlotinib/Tarceva is a small molecule inhibitor targeting EGFR, which has been validated in clinical trials enrolling GBM patients, but it has not prolonged survival[72]. Since aiming at EGFR alone does not show promising results, attempts are made to simultaneously target downstream proteins in the EGFR-signaling cascade, such as the mammalian target of rapamycin (mTOR). Several mTOR inhibitors such as rapamycin, temsirolimus, everolimus and deforolimus have been tested in trials as single or combinatorial drugs, but so far the clinical responses have been poor[73].

The fact that these treatments largely fail to improve patient outcome underscores the need of translational research and new clinical trials in order to develop new and more effective treatments for GBM.

1.4.3 Targeting hypoxic cells

As previously mentioned hypoxia has been associated with poor prognosis in many solid cancers, and insufficient oxygen levels in the tumor bed at the time when radiation is given strongly influences the response to radiotherapy[40, 74]. Attempts have been made to resensitize hypoxic tumors to radiation by different approaches, but so far none have been accessible and effective enough to become routine practice in the clinic[75]. One of the first strategies to modify the hypoxic microenvironment of tumors was hyperbaric breathing of oxygen, normally at 3 atmospheres, to increase the overall oxygen pressure in the blood[75]. Nitroimidazoles are also assessed because they mimic oxygen in the chemical process where radiation leads to creation of free radicals[75]. Hypoxic cytotoxins that act by specifically destroying hypoxic cells rather than sensitizing cells to radiation[75], have also been tested. Other approaches include targeting HIF-1 with small molecule inhibitors to prevent the whole angiogenic and survival program induced by this transcription factor in hypoxic cells. Compounds have been found which in cell-based systems inhibit HIF-1α protein synthesis, influence protein stability, reduce interactions with co-activators and ARNT or prevent binding to DNA[76]. Still, targeting hypoxia and HIFs stand out as an approach that is

extensively studied in the laboratories, but repeatedly fails translation into the clinic[75]. Testing of small molecular inhibitors in animal models and clinical trials will reveal more about how HIF functions as well as provide knowledge that can lead to development of novel compounds to treat cancer[76].

2 Aims

Based on the information provided in the previous sections, the following hypothesis and aims are outlined in the presented thesis:

2.1 Hypothesis

Hypoxia is associated with poor prognosis in many solid cancer types, and is connected to radiation resistance and resistance to chemotherapy. Cancer stem cells have also been connected to poor prognostics and reduced treatment efficacy. We therefore hypothesize that hypoxia induces stem-like traits in glioma cell lines.

2.2 Aims

I.   Establish a protocol for culturing of cells in hypoxia.

II.   Culture glioma cell lines in normoxia (21.0 % O_2) and hypoxia (2.0 and 0.5 % O_2), and investigate expression of cell line markers associated with different cell types in CNS.

III.   Investigate growth properties of glioma cell lines cultured in hypoxia compared to normoxia by looking at growth rates, cell division and apoptosis.

IV.   Investigate migration properties of glioma cell lines in hypoxia and normoxia by the use of electric cell-substrate impedance sensing.

3 Materials

Table 3.1: Cell lines

Name	Source	Catalogue nr.	Distributor
A172	Human glioblastoma	CRL-1620	ATCC[1], Manassas, Virginia, USA
LN-18	Human glioblastoma	CRL-2610	ATCC, Manassas, Virginia, USA
NCH-644	Human Glioblastoma	–	Christine Herold-Mende, Dept. of Neurosurgery, University of Heidelberg, Heidelberg, Germany
U-118 MG	Human glioblastoma, astrocytoma	HTB-15	ATCC, Manassas, Virginia, USA
U-251 MG	Human glioblastoma, astrocytoma	Unavailable	ATCC, Manassas, Virginia, USA
U-87 MG	Human glioblastoma, astrocytoma	HTB-14	ATCC, Manassas, Virginia, USA

Table 3.2: General chemicals and solutions

Chemical/Solution	Catalogue nr.	Supplier
Acetic acid, 100 %	1.00062.1000	Merck Chemicals, Darmstadt, Germany
Acetone	1.00014.1000	Merck Chemicals, Darmstadt, Germany
Agarose 3:1	50004	Lonza, Basel, Switzerland
Annexin-V conjugated to FITC	A13199	Molecular Probes (Invitrogen), Carlsbad, California, USA

---

[1] American Type Culture Collection

Benzamidine	12072	Sigma-Aldrich, St. Louis, Missouri, USA
Bovine serum albumin (BSA)	A4503	Sigma-Aldrich, St. Louis, Missouri, USA
Difco Skim Milk Powder	232100	BD Biosciences, Franklin Lakes, New Jersey, USA
Dimethyl Sulphoxide (DMSO)	D2438	Sigma-Aldrich, St. Louis, Missouri, USA
DNase	79254	Qiagen, Hilden, Germany
Dulbecco's Modified Eagle's Medium (DMEM)	D5671	Sigma-Aldrich, St. Louis, Missouri, USA
EDTA	ED2SS	Sigma-Aldrich, St. Louis, Missouri, USA
EGTA	E4378	Sigma-Aldrich, St. Louis, Missouri, USA
Ethanol, absolute	32221	Sigma-Aldrich, St. Louis, Missouri, USA
Ethidium Bromide (EtBr), 10 mg/ml	E1510	Sigma-Aldrich, St. Louis, Missouri, USA
Isopropalol	600079	Arcus Kjemi, Vestby, Norway
L-Cysteine	C7352-25G	Sigma-Aldrich, St. Louis, Missouri, USA
Leupeptin	108975	Merck Chemicals, Darmstadt, Germany
L-Glutamine	BE17605E	Cambrex, New Jersey, USA
Methanol (100%)	1060122500	Merck Chemicals, Darmstadt, Germany
Molecular biology Grade H_2O	955155025	Eppendorf AG, Hamburg, Germany
MOPS (3-morpholinopropane-1-sulfonic acid)	475898	Sigma-Aldrich, St. Louis, Missouri, USA

Materials

Na-Orthovandate	S6508	Sigma-Aldrich, St. Louis, Missouri, USA
Na-Pyrophosphate	S6422	Sigma-Aldrich, St. Louis, Missouri, USA
Non-essential amino acids	BE13114E	Cambrex, New Jersey, USA
NuPAGE 4-12 % Bis-Tris Gel	NP0322BOX	Invitrogen, Carlsbad, California, USA
NuPAGE Antioxidant	NP0005	Invitrogen, Carlsbad, California, USA
Paclitaxel	86346	Fluka, Sigma-Aldrich, St. Louis, Missouri, USA
Paraformaldehyde (PFA) powder	76240	Fluka, Sigma-Aldrich, St. Louis, Missouri, USA
Penicillin/Streptomycin	DE17603E	BioWhittacker Inc., Walkersville, Maryland, USA
Pepsin, 0.5 %, pH 1.5		Sigma-Aldrich, St. Louis, Missouri, USA
Pepstatin	516485	Merck Chemicals, Darmstadt, Germany
Plasmocin	ant-mpt	InvivoGen, California, USA
PMSF (phenylmethanesulfonyl fluoride)	P7626	Sigma-Aldrich, St. Louis, Missouri, USA
Ponceau	P3504	Sigma-Aldrich, St. Louis, Missouri, USA
Propidium iodide (PI)	P4170	Sigma-Aldrich, St. Louis, Missouri, USA
Protein Assay Dye Reagent Concentrate	500-0006	BIO-RAD, Hercules, California, USA

RNA loading dye	R0641	Fermentas, Thermo Fisher Scientific, Waltham, Massachusetts, USA
SeeBlue Plus2 Prestained Standard (1x)	LC5925	Invitrogen, Carlsbad, California, USA
Sodium fluoride (NaF)	80373	Sigma-Aldrich, St. Louis, Missouri, USA
Soduim cloride (NaCl)	S0390	Sigma-Aldrich, St. Louis, Missouri, USA
Tris Base	648310	Merck Chemicals, Darmstadt, Germany
Triton X-100	T8787	Sigma-Aldrich, St. Louis, Missouri, USA
Trypsin-EDTA 200 mg/L Versene	BE17-161E	Lonza, Basel, Switzerland
Tween 20	170-6531	BIO-RAD, Hercules, California, USA
Vectashield Mounting Solution w/DAPI	H1200	Vector Laboratories, Burlingame, California, USA
Virkon tablets for decontamination	VIRKTABS	Wilmington, Delaware, USA
β-Glycerophosphate	35675	Merck Chemicals, Darmstadt, Germany

Table 3.3: Commercial buffers

Buffer	Catalogue nr.	Supplier
Annexin binding buffer (5x): 50 mM HEPES, 700 mM NaCl, 12.5 mM CaCl$_2$, pH 7.4	V13246	Molecular Probes/Invitrogen, Carlsbad, California, USA
Dulbecco's Phosphate Buffered Saline (10x)	D1408	Sigma-Aldrich, St. Louis, Missouri, USA

Materials

NuPAGE LDS Sample Buffer (4x)	NP0007	Invitrogen, Carlsbad, California, USA
NuPAGE MOPS Running Buffer (20x)	NP0001	Invitrogen, Carlsbad, California, USA
NuPAGE Transfer Buffer (20x)	NP0006-1	Invitrogen, Carlsbad, California, USA
Phosphate buffered saline without calcium and magnesium (10x)	04-409	Bio-Whittaker/Lonza, Basel, Switzerland

Table 3.4: Buffers/solutions prepared in the lab

Buffer	Constituents
Annexin binding buffer (1x)	Annexin binding buffer (5x) diluted 1:4 in MilliQ H_2O
Blocking buffer for ICC, 0.5%	250 μg bovine serum albumine dissolved in 50 ml MilliQ H_2O, sterile filtered
Blocking buffer for western blot, 5 %	2.5 g skim milk in TBST w. Tween 0.1 %, dissolved by vortexing
Cell-freezing solution	0,5 ml DMSO, 0,5 ml 10% heat inactivated calf serum, 4 ml DMEM-ALT
DMEM-ALT	DMEM supplemented w. 10 % heat inactivated calf serum, four times the prescribed amount of non-essential amino acids, L-Glutamine, penicillin (100 μg/ml) and streptomycin (100 μg/ml)
Dulbecco's Phosphate Buffered Saline (1x)	1 volume of Dulbecco's Phosphate Buffered Saline (10x), 9 volumes of autoclaved MilliQ H_2O
Fixation reagent, 4 %	4 g lyophilized PFA in 100 ml 1xPBS

Kinexus lysis buffer	500 mM MOPS, 500 mM EDTA, 100 mM EGTA, 500 mM NaF, 10 % Triton X-100, 500 mM b-Glycerophosphate, 400 mM Na-Pyrophosphate (pH 7.0), 250 mM Na-Orthovandate, 1 mM Pepstatin, 50 mM Leupeptin, 100 mM PMSF (in isopropanol), adjusted to pH 7.2 and expanded to 20 ml with ddH_2O
Permeabilizing reagent for fixed cells, 0.5 %	250 μl Triton X-100 dissolved in 50 ml MilliQ H_2O
Ponceau S	0.1 % Ponceau S, 5 % acetic acid
Rinsing Buffer for WB (TBST)	20 ml 0.5 M Tris/HCl pH 7.5 + 75 ml 1M NaCl + 0.5 ml Tween 20. Adjusted to 500 ml with MilliQ H_2O
Running buffer for SDS-PAGE	200 ml 1x NuPAGE MOPS running buffer (20xMOPS diluted with MilliQ H_2O) and 500 μl NuPAGE antioxidant
Transfer buffer for WB	25 ml 20x NuPAGE transfer buffer, 50 ml 100 % methanol, 500 μl NuPAGE antioxidant, adjust to 500 ml with MilliQ H_2O
Tris-HCl (1M)	121.14 g Tris Base dissolved in 900 ml MilliQ H_2O, adjust pH to 7.5

Table 3.5: Plastic and paper ware

Article	Catalogue nr.	Supplier
Chromatography paper, 3 mm	3030917	Whatman International Ltd., Kent, United Kingdom
Cryo tubes	377267	Nunc, Thermo Fischer Scientific, Waltham, Massachusetts, USA

Materials

Nunc Easy flask with Nunclon Δ, 25 mm^2	156367	Nunc, Thermo Fischer Scientific, Waltham, Massachusetts, USA
Nunc Easy flask with Nunclon Δ, 75 mm^2	156499	Nunc, Thermo Fischer Scientific, Waltham, Massachusetts, USA
Parafilm "M"	PM-966	Structure Probe, Inc., West Chester, Pennsylvania, USA
Protran Nitrocellulose Transfer Membrane, 0.2 µm	10401396	Whatman International Ltd., Kent, United Kingdom
Touch N Tuff Disposable Nitrile Gloves	92-600	Ansell, Red Bank, New Jersey, USA
TPP Tissue Cell Scraper	99002	MidSci, St. Louis, Missouri, USA

Table 3.6: Primary antibodies for ICC and Western Blot

Anti-X antibody, application	Dilution	Source species and clonality	Catalogue nr.	Supplier
BrdU (ICC)	1:100	Mouse monoclonal IgG	Ab8152	Abcam, Cambridge, United Kingdom
CD133	1:20	Mouse monoclonal IgG1	AC141	Miltenyl Biotech GmbH, Bergisch Gladbach, Germany
GAPDH (WB)	1:2500	Rabbit polyclonal IgG	Ab9485	Abcam, Cambridge, United Kingdom
GFAP (ICC)	1:500	Goat polyclonal IgG	Sc-1672	Santa Cruz Biotechnology, Santa Cruz, California, USA

HIF-1α (ICC, WB)	ICC 1:500 WB 1:300	Mouse monoclonal IgG1	610959	BD Transduction Laboratories, Franklin Lakes, New Jersey, USA
Nestin (ICC)	1:500	Rabbit polyclonal IgG	Ab5922	Chemicon (Millipore), Billerica, Massachusetts, USA
βIII -tubulin (ICC)	1:100	Mouse monoclonal IgG	MAB1637	Chemicon (Millipore), Billerica, Massachusetts, USA

Table 3.7: Secondary antibodies

Secondary Antibodies	Dilution	Type/source-species	Catalogue nr.	Supplier
FITC conjugate	1:200	Goat anti-mouse IgG1	1070-02	Southern Biotech, Birmingham, Alabama, USA
HRP	1:25 000	Goat anti-mouse IgG	sc-2005	Santa Cruz Biotechnology, Santa Cruz, California, USA
HRP	1:100 000	Goat anti-rabbit IgG	sc-55226	Santa Cruz Biotechnology, Santa Cruz, California, USA
Texas Red conjugate	1:200	Goat anti-mouse IgG1	1070-07	Southern Biotech, Birmingham, Alabama, USA
Texas Red conjugate	1:200	Goat anti-rabbit IgG	4010-07	Southern Biotech, Birmingham, Alabama, USA
Texas Red conjugate	1:1000	Rabbit polyclonal anti-goat IgG	Ab 6738-1	Abcam, Cambridge, United Kingdom

Materials

Table 3.8: Primers[2] for qRT-PCR

Target gene	Primer sequence
TUBB3	Fw 5' – TTT – AGA – CAC – TCC – TGG – CTT – CG – 3'
	Rev 5' – CGC – AGA – TGT – ACG – AAG – ACG – AC – 3'
CAIX	Fw 5' – CAC – CAG – CGT – CGC – GTT – CC – 3'
	Rev 5' – TAG – GCT – CCA – GTC – TCG – GCT – ACC – 3'
CD133	Fw 5' – CAA – GAA – TTC – CGC – CTC – CTA – GCA – CT – 3'
	Rev 5' – ACC – AGG – TAA – GAA – CCC – GGA – TCA – A – 3'
GAPDH	Fw 5' – GAG – TCA – ACG – GAT – TTG – GTC – GT – 3'
	Rev 5' – GAC – AGC – TTC – CCG – TTC – TCA – G – 3'
GFAP	Fw 5' – AGA – AGC – TCC – AGG – ATG – AAA – CC – 3'
	Rev 5' – AGC – GAC – TCA – ATC – TTC – CTC – TC – 3'
Nestin	Fw 5' – TCC – AGG – AAC – GGA – AAA – TCA – AG – 3 '
	Rev 5' – GCC – TCC – TCA – TCC – CCT – ACT – TC – 3'

Table 3.9: Commercial Kits

Article	Catalogue number	Producer
iQ SYBR Green Supermix	170-8882	BIO-RAD, Hercules, California, USA
iScript cDNA kit	170-8890	BIO-RAD, Hercules, California, USA
Qiagen RNeasy Mini Kit	74106	Qiagen, Hilden, Germany
Super Signal West Pico Chemiluminescent Substrate	34080	Thermo Fischer Scientific, Waltham, Massachusetts, USA

---

[2] All primers are bought from Invitrogen, San Diego, California, USA.

Table 3.10: Hardware

Name	Catalogue number/Model	Supplier
Accuri Flow Cytometer	C6	Accuri Cytometers Inc., Ann Arbor, Michigan, USA
Asys UVM 340 Microplate Reader	G019065090	Biochrom Ltd., Cambridge, United Kingdom
CO_2 incubator	MCO-19AIC (UV)	SANYO Electric Co. Ltd., Moriguchi City, Osaka, Japan
Confocal Microscope	LSM 510 Meta	Carl Zeiss Microimaging GmbH, Oberkocken, Germany
Electric cell-substrate impedance sensing (ECIS)	ECIS-Z	Applied Biophysics Inc, Troy, New York, USA
Fluorescence microscope	Axioplan II	Carl Zeiss Microimaging GmbH, Oberkocken, Germany
Horizon58 Horizontal Gel Electrophoresis Apparatus	41060	Biometra, Göttingen, Germany
Hypoxia C-chamber	C-374	BioSpherix, Lacona, New York, USA
Luminescent Image Analyzer	LAS3000	Fujifilm Medical Systems Inc., Stamford, Connecticut, USA
Novex Mini-Cell chamber	–	Invitrogen, Carlsbad, California, USA
Peltier Thermal Cycler	PTC-200	BIO-RAD, Hercules, California, USA

Materials

Roche's Real time PCR system	LightCycler 480	Roche, Basel, Switzerland
Vibra Cell Sonicator	VC130	Sonics & Materials Inc., Newton, Connecticut, USA

Table 3.11: Software

Program	Version	Supplier
Adobe Photoshop	CS5	Adobe Systems Inc., San Jose, California, USA
DigiRead	1.0.2.0	Biochrom Ltd., Cambridge, United Kingdom
ECIS software	1.2.2	Applied Biophysics Inc, Troy, New York, USA
Flow-Jo	9.3.1	Tree Star Inc., Ashland, Oregon, USA
Microsoft Office Excel	2003	Microsoft Corporation , Redmond, Washington, USA
QuantPrime qPCR Primer designing tool	2011	Free online program by Samuel Arvidsson, University of Potsdam, Potsdam, Germany
Real Time PCR analysis software	LCS480	Roche, Basel, Switzerland

4 Methods

All procedures were performed at room temperature unless otherwise stated.

4.1 Cells

4.1.1 Cell culturing

Glioma cell lines were kept at $37^{o}C$ in tissue culture incubators at 100 % humidity with 5 % CO_2 and 95 % air. The cells were grown as monolayers in 75 cm^2 culture flasks (Nunc, Thermo Fischer Scientific, Waltham, Massachusetts, USA) to 80 % confluency before they were trypsinized and passaged as follows: Old medium was removed before the cells were washed twice with 1x phosphate buffered saline (1xPBS, Sigma Aldrich, St. Louis, Missouri, USA). The cells were detached by incubation at $37^{o}C$ in Trypsin-EDTA (Lonza, Basel, Switzerland) for 3-5 minutes. Trypsin was inactivated by adding supplemented Dulbeccos Modified Eagles Medium (DMEM-ALT (table 3.4), Sigma Aldrich, St. Louis, Missouri, USA). Excessive cells were discarded and 15 ml fresh DMEM-ALT was added. Passage number was registered each time the cells were passaged. All work with cells was carried out wearing protective gloves and coat in a laminar flow bench (SANYO Electric Co, Osaka, Japan) that was sterilized with 70 % ethanol before and after use. Equipment used in the laminar flow bench was sterilized with 70 % ethanol or microwaved at full effect for two minutes. Cells were monitored using an inverted light microscope.

4.1.2 Cryopreservation of cells

Cells were frozen down for cryopreservation as soon as the first passaging of newly thawed cells. When approximately 80 % confluent, cells were trypsinized as previously described and transferred to a 15 ml centrifuge tube. The cell suspension was then centrifuged at 700 g for five minutes. After discarding the supernatant, pelleted cells were resuspended in 2 ml freezing solution (table 3.4), and then distributed into two cryotubes. Tubes were marked with cell line, passage number, date, and name of owner and placed in an isopropanol container for about 24 hours and frozen down to $-80^{o}C$. Isopropanol ensures a slow decline in temperature of about $1^{o}C$ per minute. The cryotubes were then placed in the N_2-tank for cryopreservation at $-196^{o}C$. Cryopreservation was done in order to keep a batch of cells from the same passage as reserve. If cells are kept in culture for a long time, typically more than 25 passages or two-three months, the may change character due to genetic drift, selection or cross

contamination[77]. To achieve comparable results over time, it is therefore important to perform experiments within the same range of passages.

4.1.3 Thawing of cells

Cells were collected from the N_2-tank and thawed by placing the cryotubes in a $37^{\circ}C$ water bath. Immediately after thawing, the cell suspension was transferred to a culture flask containing 15 ml DMEM-ALT. After 24 hours incubation, the medium was changed to remove remnants of freezing solution which may otherwise harm the cells.

4.1.4 Counting cells

In some of the experiments, cells were counted prior to seeding or during the experiment. A Bürker chamber was used for determination of cell concentration. 10 µl of cell suspension was pipetted into the chamber. The chamber has a grid system of 3x3 large squares each with a volume of 10^{-4} ml. Cells in three large squares were counted and divided by three to achieve an average number of cells in one square. This number was multiplied by 10^4 to give the number of cells in one ml.

4.2 The hypoxia chamber

The chamber used for the hypoxia experiments was the C-chamber from BioSpherix Ltd (Lacona, New York, USA). The dimensions of the chamber are 35x30x20 cm, which makes it fit into a warming cabinet to ensure physiological temperatures of $37^{\circ}C$. The chamber has two sensors, one that senses the CO_2 concentration and one that senses the O_2 concentration. Two regulators control the gas flow into the chamber through tubes connected to the back of the chamber. One regulator controls the flow of CO_2 and one controls the flow of N_2 into the chamber. Since it is a low oxygen chamber, N_2 is pumped into the chamber to replace O_2. The CO_2 concentration was set to 5.0 % as in standard tissue culture incubators. The hypoxia experiments were performed at 2 % and 0.5 %, and the O_2 concentration was set to the corresponding values. The sensors were calibrated using a mixture of 90 % N_2 and 10 % CO_2, 100 % N_2 and normal air (21 % O_2).

4.2.1 Preparation of hypoxia conditioned cells for immunocytochemistry

All experiments were done in 0.5 % O_2 (from now on called hypoxia) and in the standard tissue culture incubator (from now on defined as normoxia). Only ICC was performed in hypoxia at 0.5 % *and* 2 % O_2. Cells were seeded on coverslips at a density of 80,000 cells per well and fixed after 24 hours. Cells were also seeded at a density of 30,000 cells per well and fixed after four days. The plate was placed in the hypoxia incubator for the desired time. Fixation was done immediately after incubation (as explained in chapter 4.3.2) and stored in PBS at 4°C until use.

Cells were also grown in culture flasks in the hypoxia chamber. These flasks were used to prepare cells that were conditioned with hypoxia for a longer period of time. For the ICC experiments cells were fixed after eight days, twelve days, and after four weeks in hypoxia. Two days before each fixation cells were collected from the cell flask and seeded onto coverslips in 24-well plates. The well plates were subsequently put back into the hypoxia chamber and incubated for two more days until fixation.

4.2.2 Other experiments with hypoxia conditioned cells

Cells were grown in culture flasks until the time point when RNA isolation, protein extraction or preparation for flow cytometry was performed. The ECIS equipment (chapter 4.6.5) was also installed inside the hypoxia chamber. For the experiments in hypoxia, one or more of five different glioma cell lines U-251, A172, U-118, LN-18 and U-87 (table 3.1) were used. For each experiment, control cells were always incubated in normoxia for the same period of time and were exposed to the same treatment.

4.3 Immunocytochemistry

4.3.1 Immunocytochemistry

Immunocytochemistry (ICC) is a technique for detecting a protein of interest inside or on the membrane of cells. The protein is identified by using an antibody conjugated to a fluorescent tag – a fluorophore. Immunostaining can then be investigated using different techniques, for example fluorescence microscopy and confocal microscopy. One can distinguish between direct and indirect ICC. In direct ICC, only a primary fluorophore-conjugated antibody is

used. In indirect ICC, a primary antibody is allowed to bind to the target protein first, and then a secondary fluorophore-conjugated antibody binds to the primary antibody. Indirect ICC is more sensitive because several secondary antibodies can bind to a single primary antibody, thus enhancing the signal.

4.3.2 Preparation of cells

For immunostaining, cells were seeded on sterile 10 mm coverslips in a 24-well plate. Approximately 50,000 cells were seeded in each well, and then incubated with DMEM-ALT for the desired time. Cells were then washed twice with 1xPBS and fixed using 4 % paraformaldehyde (PFA, fixation reagent, table 3.4) as follows: Each coverslip was covered in PFA for 10 minutes. PFA was removed and the cells were permeabilized with 0.5 % Triton X-100 (Zigma-Aldrich) for four minutes. Triton X-100 was then removed and cells were washed three times with 1xPBS and stored in 1xPBS at 4°C until use.

Non-adherent cells that were used to perform ICC were cytospun to object glass slides for 3 minutes at 800 g. Cells were then fixed in ice cold acetone for 10 minutes and stored in -20° C until use.

4.3.3 Immunostaining

The procedure for immunostaining was done at the lab bench. Staining was done by pipetting 30 µl droplets of the various solutions onto a parafilm-covered bottom of a flat plastic box. The coverslips were moved from droplet to droplet using tweezers. The cells were first incubated in blocking buffer for ICC (table 3.4) for 15 minutes to prevent unspecific binding of the antibody. Then the cells were incubated with primary antibody diluted in blocking buffer for 45 minutes at 37°C. A wet paper towel in the box prevented the coverslips from drying out. After incubation, cells were washed with 1xPBS 2x3 minutes. Incubation with secondary antibody diluted in blocking buffer was done for 45 minutes at 37°C. The coverslips were then washed 3x3 minutes before dipped in MilliQ water to remove salts. Finally the coverslips were mounted onto object glasses with 5 µl Vectashield mounting solution containing DAPI (Vector Laboratories, Burlingame, California, USA). DAPI stains the nucleus of the cell by binding to DNA. The mounting solution was allowed to dry for at least one hour before it was secured with nail polish. Every step from incubation with

secondary antibody and onwards was done without bench light. All immunostainings were done with negative controls by omitting the primary antibody.

4.3.4 Confocal imaging

In a regular fluorescence microscope, the whole specimen is excited at the same time, and this gives a certain background and blur in the image. The principle of confocal imaging is the use of a pin hole to avoid detection of emitted light that is outside the focal plane. The pin hole is situated on the other side of two lenses where the focal point creates an image. The pin hole and focal point are positioned *confocal* to each other, hence the name of the microscope. This allows only the emitted light from the focal point, which has the highest intensity, to be detected while all other light is excluded. When light is emitted by the specimen and focused through the pin hole it is detected by the photomultiplier tube connected to a computer. Only one spot (pixel) in the specimen is detected at a time, and the computer builds up an image as a chosen number of pixels detected. The confocal microscope used to examine and image the ICC experiments performed in this project was the Zeiss LSM 510 Meta (Carl Zeiss, Oberkochen, Germany) located in the Molecular Imaging Center (MIC), Bergen. Zeiss LSM 510 Meta is equipped with several lasers, of which the UV laser was used to excite at 358 nm (DAPI), the Argon laser was used to excite at 488 nm (FITC) and the HeNe laser was used to excite at 543 nm (Texas Red).

4.4 SDS-PAGE and Western Blotting

SDS-PAGE (sodium dodecyl sulfate polyacrylamide gel electrophoresis) is used to separate proteins according to size. This is achieved through the use of SDS, which denatures the proteins so they all have a linear shape in addition to giving them a negative charge. Like that they all migrate towards the positive pole in the PAGE, and they are separated on the gel by their size. The separated proteins can be transferred to a membrane and thereafter be detected by the use of epitope specific antibodies that bind to the proteins on the membrane.

4.4.1 Protein isolation

Cell flasks were kept on ice while they were washed twice with 3 ml ice cold 1xPBS. 150 µl Kinexus protein lysis buffer (with Triton X-100 to disrupt cell membranes, protease inhibitors

to protect from protein degradation and phosphatase inhibitors that protect from protein dephosphorylation) was added, and a cell scraper was used to loosen the cells. The cell-lysis buffer suspension was transferred to a 1.5 ml eppendorf tube and incubated for 10 minutes on ice. A sonicator (Sonics Vibra Cell, Newton, Connecticut, USA) was used at 20 Hz for 3x2 seconds to further disrupt the cell membrane and homogenize the intracellular content. The samples were then centrifuged for 30 minutes at $4^{o}C$ and maximum speed (16,000 g) in an eppendorf microcentrifuge. The supernatant which contains the protein was transferred to a new 1.5 ml eppendorf tube and stored at $-80^{o}C$ until use.

4.4.2 Determination of protein concentration

1.5 µl of each sample was mixed with 788.5 µl MilliQ H_2O, 10 µl lysis buffer and 200 µl dye reagent concentrate for protein assay (BIO-RAD, Hercules, California, USA) to a final volume of 1000 µl per sample. For each sample 200 µl of this solution was transferred to a 96 well plate for spectrophotometric analysis at 595 nm (ASYS UVM 340 with DigiRead Microplate Instrumentation Control). A standard curve for determination of protein concentration was made by measuring absorbance at 595 nm for a series of six dilutions of BSA (0, 1, 2, 4, 6 and 10 µg). Microsoft Office Excel (Microsoft Corporation, Redmond, California, USA) was used for the calculations and interpolations on the standard curve.

4.4.3 SDS-PAGE

Samples were prepared to a final volume of 18 µl as shown in table 4.4.3. The samples were boiled at $70^{o}C$ for 10 minutes. The Novex mini-cell gel chamber (Invitrogen, Carlsbad, California, USA) was used together with a 12-well NuPage 4-12 % Bis-Tris gel (Invitrogen). The inner chamber was assembled first and filled with 200 ml 1x NuPage MOPS SDS Running Buffer with 500 µl antioxidant (Invitrogen). The wells of the gel were flushed with running buffer before loading to remove air. 7 µl SeeBlue Plus2 Prestained Standard (Invitrogen) and 15 µl of each sample mixture were loaded and the outer chamber filled with 1x running buffer. The gel was run for 50 minutes at 200 V.

Table 4.4.3: Loading mixture for SDS-PAGE

Sample	10 µg protein (in µl)	10X DTT (µl)	4X LDS buffer (µl)	MilliQ H_2O (µl)	Total volume (µl)
1	x	1.8	4.5	x	18

4.4.4 Blotting

Transfer buffer was prepared as described in table 3.4. The nitrocellulose membrane, sponges and filter paper were soaked in transfer buffer before assembling with the gel. The transfer chamber was filled with transfer buffer and the outer chamber with MilliQ H_2O. Blotting was run for 80 minutes at 30 V.

4.4.5 Ponceau S staining

After blotting, the nitrocellulose membrane was washed in MilliQ H_2O. The membrane was incubated for seven minutes with ponceau stain to verify that the protein had been transferred to the membrane. Ponceau S is a red dye that binds to proteins. The binding is reversible, and after staining it is easily washed off with MilliQ H_2O.

4.4.6 Blocking and antibody incubation

Blocking buffer for western blot was prepared from 2.5 g skim milk powder in 50 ml rinsing buffer (materials table 3.4). The blot was then blocked with gentle agitation for 1 hour in room temperature. Primary and secondary antibodies were diluted to the desired dilution in blocking buffer. The membrane was incubated with primary antibody solution with agitation over night (4^oC). The blot was then washed with rinsing buffer on a shaking board for 4x10 minutes before incubation with secondary antibody solution for 1.5 hours with gentle agitation (room temperature). The blot was washed in rinsing buffer again for 4x10 minutes on a shaking board.

4.4.7 Chemiluminescence

Blots were developed with the Super Signal West Pico Chemiluminescent Substrate (Thermo Fisher Scientific, Waltham, Massachusetts, USA). The kit contains an enhanced

Methods

chemiluminescent substrate for antibody conjugated horseradish peroxidase (HRP). The blots were allowed to absorb the substrate for five minutes before excess liquid was removed. The development was done with a luminescent image analyzer (Fujifilm Medical Systems Inc., Stamford, Connecticut, USA).

4.5 qRT-PCR

qRT-PCR (quantitative reverse transcriptase polymerase chain reaction) is based on the standard PCR-reaction. The additional feature of qRT-PCR is the use of an intercalating fluorescing dye from which the signal increases throughout the reaction. This is used to follow the amplification and to quantify the starting amount of DNA.

4.5.1 RNA isolation

Cells were washed twice with 1xPBS before incubation at 37°C with 0.5 ml trypsin for 3-5 minutes. Trypsin was inactivated by adding 3 ml DMEM-ALT and the cells transferred to a 15 ml centrifugation tube and spun down at 700 g for 5 min. The supernatant was removed and the cells were washed in 1xPBS and spun down again at 700 g for 5 minutes. RNeasy Mini Kit (Qiagen, Hilden, Germany) was used for RNA extraction according to the manufacturer's manual.

RNA was isolated three times from glioma cell lines both maintained in normoxia, and incubated in hypoxia at 0.5 % O_2 for eight days.

4.5.2 Determination of RNA concentration and quality

RNA concentration was determined with the NanoDrop1000 Spectrophotometer (Thermo Fisher Scientific). The RNA quality was reassured with agarose gel electrophoresis. 2 µl of RNA was run with 2 µl 2x RNA loading dye (Fermentas, Thermo Fisher Scientific) on a 1 % agarose gel with ethidium bromide (Zigma-Aldrich) at 90 V for 35 minutes. The bands were visualized using an UV-imager (Fujifilm Medical Systems Inc., Stamford, Connecticut, USA). If the RNA is intact and no genomic DNA is present in the samples, two distinct bands corresponding to the 18S and 28S ribosomal subunits are visual (figure 5.1.3.1).

4.5.3 cDNA synthesis

cDNA was synthesized from 250 ng RNA with the iScript cDNA synthesis kit (BIO-RAD, Hercules, California, USA). To minimize the use of reagents, the volumes indicated in the protocol were halved. The Peltier Thermal Cycler (BIO-RAD) was used for the cDNA synthesis with the reaction set up and PCR program as shown in table 4.5.3 below.

Table 4.5.3: Raction set up (a) and PCR program (b) for cDNA synthesis

a) Reagents	µl
5X cDNA synthesis kit buffer	5
iScript enzyme mixture	0,5
RNA sample	x
Nuclease-free water	x
Total volume	10

b) cDNA program	^{o}C
5 min	25
30 min	42
5 min	85
Hold	4

After cDNA synthesis the cDNA was diluted 1:10 by adding 90 µl molecular grade water and stored at -80°C until use.

4.5.4 qRT-PCR

For qRT-PCR the iQ SYBR Green Supermix kit (BIO-RAD) was used with the setup shown in table 4.5.4. A master mix was made from the SYBR Green Supermix, primer pairs and H$_2$O before distributing it into the wells, and then cDNA was added.

Table 4.5.4: Reaction setup (a) and program for qRT-PCR (b)

a) Reagent	µl
iQ SYBR Green Supermix	10
Primer pairs (1 µM)	4
cDNA (template)	1
Molecular grade H$_2$O	5
Total volume	20

b) qRT-PCR program	^{o}C	Time
Initial denaturation	95	5 min
Denaturation	95	10 sec
Annealing	60	10 sec
Extension	72	10 sec
Final extension	72	5 min
Hold	4	for ever

Methods

qRT-PCR was performed in 96/384 well plates on Roches LightCycler 480 Plate-based Real-time PCR System (Roche, Basel Switzerland). Each gene was investigated in three isolated RNA samples, and each sample was run in triplets.

The qRT-PCR results were analyzed with the LCS480 software (Roche) and exported to Excel for $\Delta\Delta C_T$-analysis. Student's t-test was used to test for statistical significance.

4.6 Quantification of proliferation, migration and cell death

4.6.1 Growth curves

To examine how the cells would grow in hypoxia compared to normoxia, growth curves for three cell lines (LN-18, U-251 and U-87) were established. For each cell line 10,000 cells were seeded in each of six small cell flasks. Three of the flasks were incubated in the hypoxia chamber and three in the standard tissue incubator. Cells in one flask were counted on the days three, six and nine, respectively. The number of cells in each flask was determined with the Bürker chamber and the numbers plotted in Excel to display them as a growth curve. The experiment was repeated three times.

4.6.2 BrdU-pulsing and S-phase quantification

Bromodeoxyuridine (BrdU) is a thymidine analogue complementary to adenosine. When supplied to the cell medium (pulsing) it is taken up by the cells. BrdU is then utilized by the cells during DNA synthesis in the S-phase of the cell cycle and is replacing thymidine. Immunocytochemistry can be used to visualize the cells that have incorporated BrdU. In our experiment cells were incubated in hypoxia for nine days, the two last on coverslips. The cells were then pulsed with BrdU (Abcam, Cambridge, UK) and incubated for 45 minutes in 37°C. Cells in normoxia were used as a control. The cells were fixed in 4 % PFA according to the protocol for ICC (chapter 4.3.2). Before incubation with the primary anti-BrdU antibody, 3 µl DNase (1 U/µl, Qiagen) was added to the antibody solution. This was done to denature the DNA strands to enable the antibody to bind to the incorporated BrdU. A FITC-conjugated secondary antibody (table 3.7) was then added in order to investigate the cells using fluorescence microscopy. DAPI was used as nuclear stain. Cells on ten different spots on the coverslip were counted, and the percentage of BrdU-positive cells quantified.

4.6.3 Flow cytometric analysis of the cell cycle distribution

Cell cycle analysis by flow cytometry (FCM) can be used to assess the fraction of dividing cells in a collected cell sample. The analysis can also be used to detect aneuploidity, typically seen in cancer cells. Forward scatter is used to detect the size of each event passing the laser beam. Since the size will be proportional to the amount of DNA, two main populations will come up, one with nuclei from cells that are in the G_1-phase and one with nuclei from cells that are in the G_2-phase. Events with other amounts of DNA than these two will distribute around these two peaks. Below the G_1-peak one finds the sub-G_1 nuclei from debris and dead cells. The S-phase nuclei will be between the G_1 and G_2 peak. Aneuploid cells will give a shift in the peaks along the x-axis compared to the normal cells.

Before cell cycle analysis 200,000 cells from the LN-18 cell line were seeded in each well in a six well plate and incubated in hypoxia for three days. Cells were trypsinized and collected by centrifugation at 700 g for 5 minutes. The supernatant was discarded and the pellet washed in 5 ml 1xPBS and centrifuged again at 700 g for 5 minutes. The supernatant was removed and the cells were fixed by adding 6 ml ice cold (-20°C) absolute ethanol drop by drop while vortexing. Fixed cells were spun down at 900 g for 5 minutes and the supernatant was removed. Cells were resuspended in 3 ml 0.5 % pepsin (Sigma-Aldrich) in PBS without calcium (pH 1.5, Bio-Whittacker/Lonza) and incubated for 15 minutes in a water bath (37°C). The suspension was spun down at 900 g for 5 minutes and the supernatant carefully removed. The pellet was washed in 5 ml 1xPBS without calcium and magnesium and spun down at 900 g for 5 minutes. The supernatant was carefully removed and 100 µl RNase (1 mg/ml) in PBS and 300 µl propidium iodide (PI, 50 µg/ml, Sigma-Aldrich) were added. The solution was vortexed and incubated for 30 minutes at room temperature. The same procedure was used to prepare control cells in normoxia and the experiment was done twice.

4.6.4 Annexin-V assay for flow cytometric quantification of cell death

Phosphatidylserine (PS) is a negatively charged phospholipid found in the inner leaflet of the plasma membrane of live cells. When a cell enters apoptosis, translocase enzymes that are responsible for maintaining asymmetry in the lipid bilayer are inactivated. At the same time scramblases that exchanges random lipids between the lipid bilayers are activated. The result is externalization of PS in apoptotic cells. Annexin-V is a human anticoagulant with a high

affinity for PS. FITC conjugated Annexin-V can therefore be utilized to detect apoptosis *in vitro* as done here by flow cytometry. Because propidium iodide does not permeate the cell membrane, PI was used to distinguish early apoptotic cells from late apoptotic and necrotic cells, whose nuclei will become stained by PI.

For the Annexin-V assay, 200,000 cells from the cell line LN-18 were seeded in each well in a six well plate and incubated in hypoxia for three days. Cells were trypsinized and collected by centrifugation at 1000 g for five minutes. In order to include dead cells floating in the medium at the moment of harvest, the old medium was saved and added again to inactivate the trypsin. The sample would then comprise both dead and alive cells from before harvesting. Cells were washed in 1xPBS and centrifuged at 1000 g for 5 minutes. The pellet was resuspended in 100 µl Annexin-V binding buffer (table 3.4). Two samples were used to prepare for color compensation in the flow cytometric analysis, one was stained only with PI (100 µl, 1 µg/ml) and one was stained only with FITC conjugated Annexin-V (5 µl, Molecular Probes, Invitrogen). One sample was also kept unstained. Samples for the apoptosis assay were stained both with PI and with FITC conjugated Annexin-V. Samples treated with the cytostatic drug Paclitaxel (Fluka, Sigma-Aldrich) were used as a positive control to ensure that the apoptosis assay had worked. Before analysis the samples were incubated in room temperature for 15 minutes. The same procedure was used to prepare control cells in normoxia and the experiment was done twice. The samples were analyzed on the Accuri C6 flow cytometer (Accuri Cytometers Ltd., Ann Arbor, Michigan, USA).

4.6.5 Wound healing assay with ECIS

Electric cell-substrate impedance sensing – ECIS (Applied BioPhysics Inc., Troy, New York, USA) is based on specialized eight well arrays with gold-covered 250 µm electrodes with a small alternating current. The cell membrane acts as an insulator to the current, and as the cells seeded into the wells increase in numbers, the resistance to the current increases proportionally. The array is connected to electronics and computer software that is used to detect the changes in resistance and display the collected data as a line graph.

Here, the ECIS was used to perform a wound healing assay to compare migration properties of cells in normoxia and hypoxia. The cell lines U-251 and LN-18 were chosen for the experiment. Before use, the electrode-array was incubated with 200 µl of 10 mM L-cysteine

(Sigma-Aldrich) solution for 10 minutes in 37°C. This was to cover any oxidized parts of the electrode, that otherwise could influence the cells. The L-cysteine solution was removed before seeding 400 µl cell suspension containing 100,000 cells into each well. The array was incubated for one hour to allow the cells to attach before connecting it to the electronics. The current used for continuous measurements of impedance was set to 32 kHz and data was collected every five minutes. When the cell layer approached confluency, the wounding was performed by applying 48 kHz to the cells at amplitude 2.5 V for 20 seconds. A dramatic drop in impedance would confirm that wounding had taken place, and the time was measured until the impedance had reached the same level as before wounding. The experiment was performed in hypoxia and normoxia sequentially.
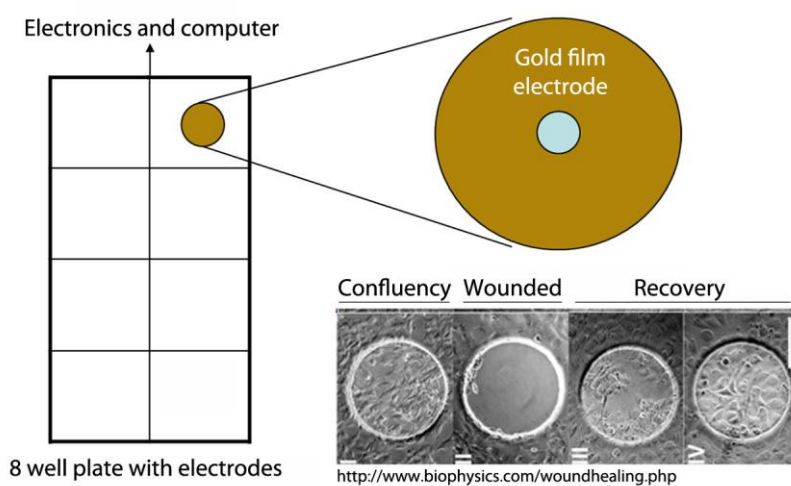

Figure 4.6.5: Schematic overview of the ECIS equipment. Cell density measurements and wounding is taking place on the 250 µm electrode indicated in blue.

5 Results

In the present study, five glioma cell lines (A172, LN18, U87, U118, U251) were investigated with respect to their expression of the cell line markers CD133, Nestin, β-III tubulin and GFAP under hypoxic and normoxic conditions. Some cell lines in the panel were chosen in order to further explore aspects of glioma cell behavior, including proliferation, apoptosis and migration in hypoxia at 0.5 % oxygen compared to normoxia.

5.1 A hypoxic environment was confirmed by stabilization of the transcription factor HIF-1α and upregulation of its downstream target CAIX

5.1.1 ICC confirms nuclear HIF-1α expression

Initially, immunocytochemistry (ICC) was performed on a panel of five glioma cell lines to investigate whether stabilization of HIF-1α takes place in the hypoxic environment created in the hypoxia chamber used (chapter 4.2, n = 2).
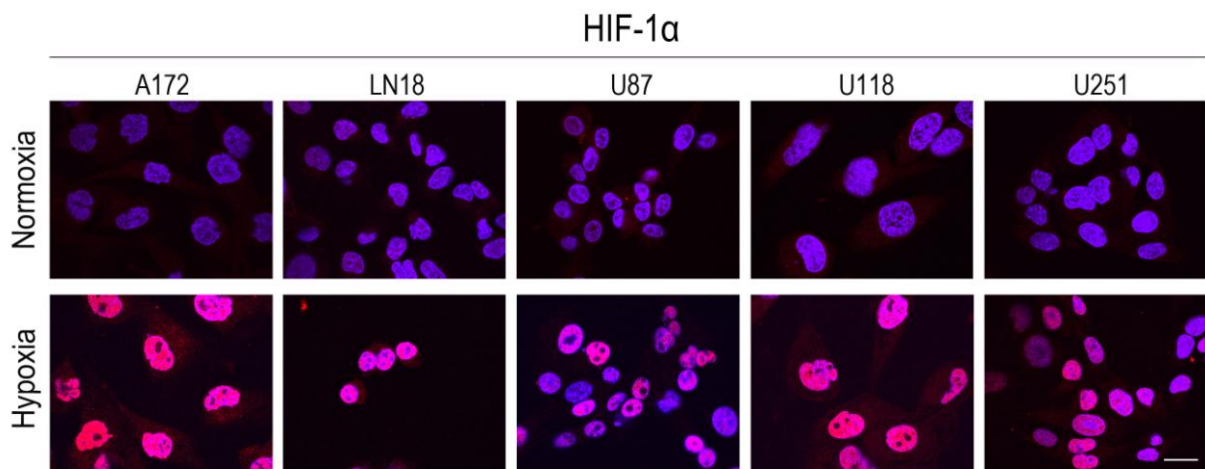

Figure 5.1.1.1: Upper panels show confocal images of different glioma cell lines immunostained for HIF-1α as indicated in 21 % oxygen. Lower panels show corresponding immunostainings for HIF-1α after incubation in 0.5 % oxygen for 24 hours. Scale bars = 20 μm, nuclear counterstaining: DAPI (blue), HIF-1α: Texas Red (red).

Under normoxic conditions, we observed no staining for HIF-1α, neither in the nuclei nor in the cytoplasms. (Figure 5.1.1.1, upper panels). However, when cultured for 24 hours in hypoxia at 0.5 % oxygen nuclei in the same cell lines stained uniformly red (Figure 5.1.1, lower panels), indicating the presence of HIF-1α. Confocal imaging, which only displays

signals from one focal plane at a time, confirmed that HIF-1α was translocated to the nucleus and not other cellular compartments which were superimposed on the nuclei.

Also, ICC for HIF-1α was performed on cells incubated in hypoxia for 24 hours at 2 % oxygen (Figure 5.1.1.2, upper panels, representative images). In 2 % oxygen nuclei also stained red, although the intensity of nuclear staining was slightly weaker than after incubation in hypoxia at 0.5 % oxygen.
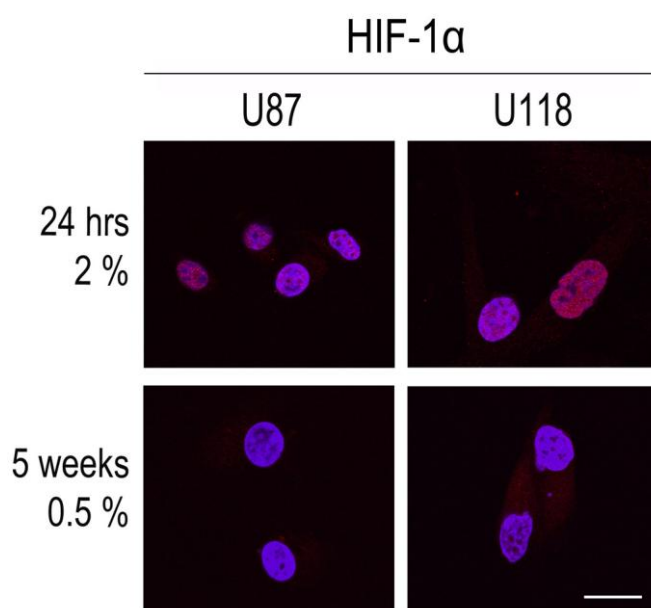

Figure 5.1.1.2: Confocal images of glioma cell lines immunostained for HIF-1α on cells incubated in hypoxia at 2 % oxygen for 24 hours (upper panel), and on cells incubated in hypoxia at 0.5 % oxygen for five weeks (lower panel). Representative images are shown for two of the cell lines, n = 2. Scale bars = 20 μm, DNA = DAPI (blue), HIF-1α = Texas Red (red).

Additionally, ICC was performed on the same panel of cell lines after culturing them in hypoxia at 0.5 % oxygen for five weeks (figure 5.1.1.2, lower panels, representative images). After five weeks, HIF-1α was not detectable in the nucleus anymore, in contrast to what was seen after 24 hours in hypoxia.

5.1.2 Western blotting of HIF-1α

In order to further confirm the stabilization of HIF-1α in hypoxia, we also performed western blotting. In accordance with the ICC, the protein for western blotting was isolated after incubating cells in small culture flasks for 24 hours in hypoxia at 0.5 %. Proteins from normoxic cells was isolated after maintaining cells in a standard incubator with 21 % oxygen as control (n = 1).
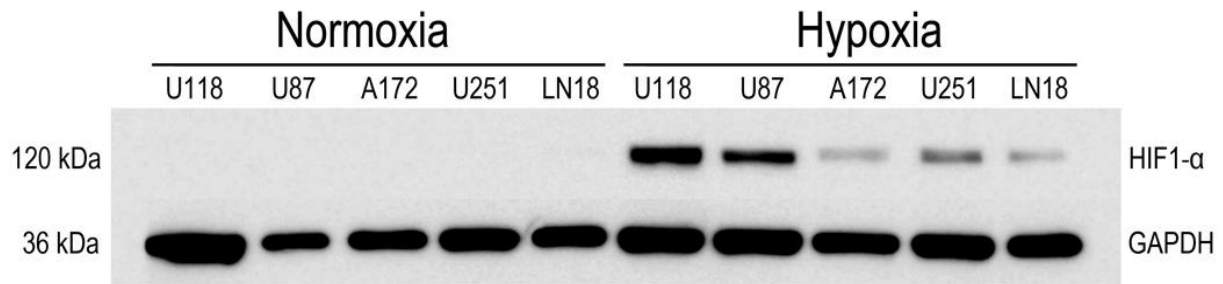

Figure 5.1.2: Western blotting of protein lysates from the panel of cell lines maintained in normoxia and after incubation in hypoxia for 24 hours. The five left lanes are the samples from normoxia, and the five right lanes represent the same cell lines cultured in hypoxia at 0.5 % oxygen. GAPDH (40 kDa) was used as an internal loading control.

The HIF-1α subunit is detected at 120 kDa, and when cultured in normoxia only (figure 5.1.2, left), cell lysate gave no visible band corresponding to the HIF-1α protein subunit. On the other hand, 24 hours incubation in hypoxia at 0.5 % oxygen (figure 5.1.2, right) produced bands at 120 kDa in all cell lines. However, the amount of HIF-1α protein varied between the different cell lines after incubation in hypoxia.

5.1.3 Expression of CAIX investigated by qRT-PCR

Carbonic anhydrase IX is a transcriptional target of HIF-1α, and is therefore expected to become upregulated in hypoxia. Here, CAIX expression was investigated by qRT-PCR to validate a transcriptional response in the cells under hypoxic conditions, and to corroborate the findings done by ICC and western blotting of HIF-1α (chapter 5.1.1 and 5.1.2, n = 3). Figure 5.1.3.1 shows a representative picture of RNA samples run on an agarose gel for RNA quality control (chapter 4.5.2). The isolated RNA was used for investigation of CAIX and cell line marker expression.
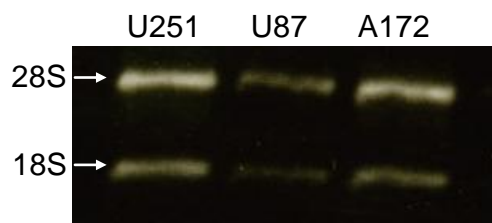
Figure 5.1.3.1: A representative picture of RNA on an agarose gel as aquality control. The bands representing the two ribosomal subunits (28S and 18S) indicate good RNA quality when they are distinct and the 28S band has approximately the double intensity of 18S.
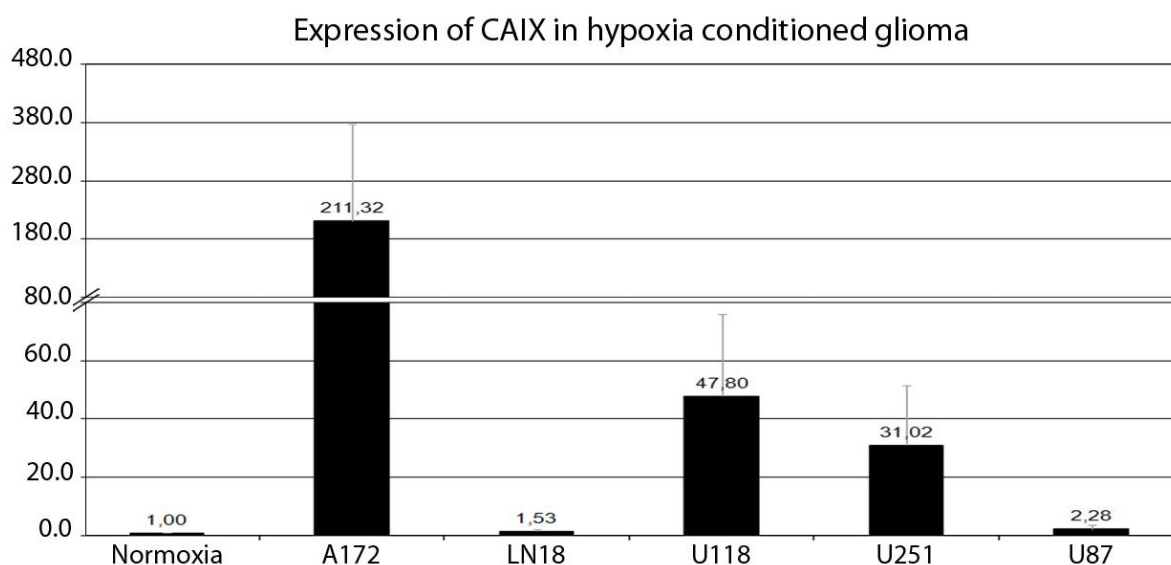

Figure 5.1.3.2: qRT-PCR results for CAIX displayed as fold change of mRNA levels in cells cultured in hypoxia at 0.5 % oxygen for eight days compared to mRNA levels of normoxic cells which are set to one. Standard error of the mean is indicated for each sample.

All five cell lines showed an upregulation, although not significant, of CAIX in hypoxia. The magnitude of upregulation varied considerably between the different cell lines. It is evident from figure 5.1.3.2 that A172 (p = 0.289) had the highest upregulation of CAIX in hypoxia after eight days incubation, while U118 (p = 0.153) and U251 (p = 0.347) also expressed higher amounts of CAIX when cultured in hypoxia for eight days. U87 (p = 0.324) and LN18 (p = 0.061) show a slight upregulation of CAIX in hypoxia.

5.2 Expression of cell line markers

GBMs are heterogeneous tumors with cells expressing markers of different CNS cell lineages. It is known that portions of GBM cells express markers associated with stem cells[56]. In order

Results

to investigate whether hypoxia could induce stem cell features in cultured glioma cell lines, expression of four different cell line markers was investigated using ICC and qRT-PCR. The markers CD133, Nestin, GFAP and βIII-tubulin were chosen because they represent different stages of maturity and lines of differentiation. CD133 and Nestin are markers of neuronal stem cells whereas GFAP and βIII-tubulin are expressed by mature astrocytes and neurons, respectively. 1.5 % oxygen is defined as tumor hypoxia[79, 80]. Furthermore 1.5 – 2 % oxygen is reported to activate HIF-1α at its half maximal activity, whereas HIF-1α reaches its maximal activity at 0.5 % oxygen[81]. Therefore, oxygen concentrations for the hypoxia experiments were set to 2 % and 0.5 %.

5.2.1. Expression of cell line markers in hypoxia – qRT-PCR

To quantitatively assess the expression of cell line markers, the expressions of CD133 (results not shown), Nestin, βIII-tubulin and GFAP were examined in hypoxia and normoxia by qRT-PCR. As for assessment of CAIX expression, RNA was isolated from glioma cell lines cultured in hypoxia at 0.5 % for eight days in order to perform qRT-PCR, and fold change was calculated by comparison to expression in normoxia (n = 3).
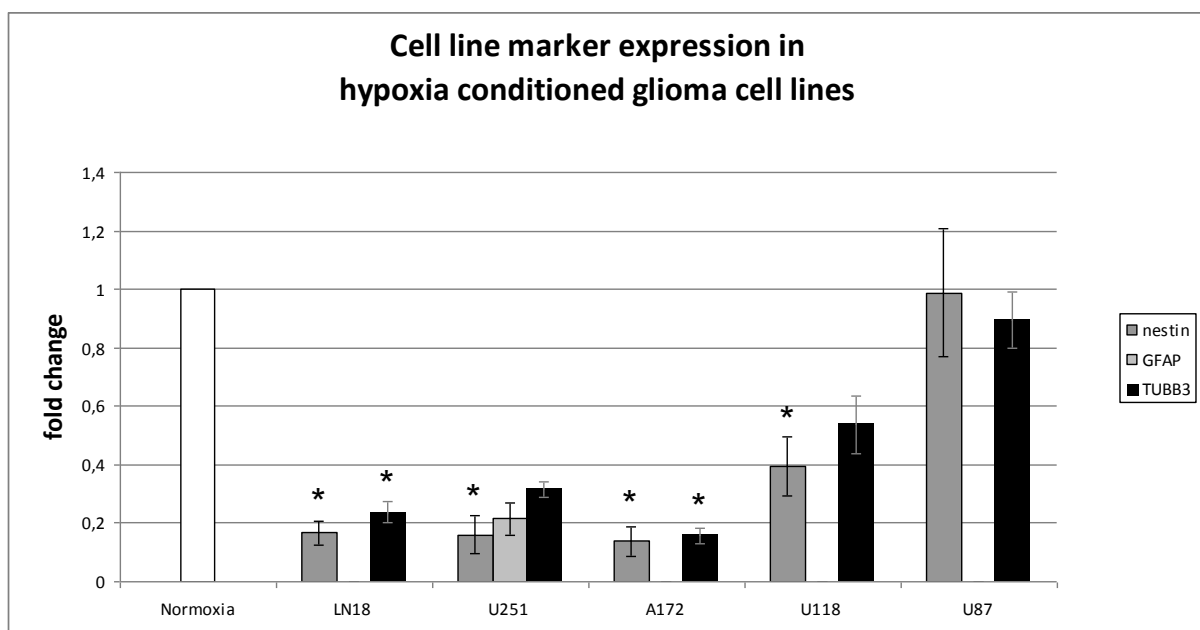

Figure 5.2.1: qRT-PCR results for Nestin, GFAP and βIII-tubulin (TUBB3). Results are displayed as relative expression by fold change of mRNA levels of cells cultured in 0.5 % oxygen for eight days compared to cells maintained in normoxia, with normoxic gene expression set to one. Standard error of the mean is indicated together with an asterisk for those results that display statistical significance (p ≤ 0.05). U251 is the only cell line expressing GFAP.

All markers investigated were downregulated after eight days in hypoxia at 0.5 % when compared to gene expression in normoxia (figure 5.2.1). Still, not all markers were significantly downregulated in hypoxia. U251 is the only cell line expressing GFAP, and according to qRT-PCR results for hypoxia, GFAP was downregulated to ca. one fifth of normoxic expression levels (p = 0.055). All cell lines were negative for CD133 also after eight days incubation in hypoxia. Interestingly, Nestin and βIII-tubulin showed similar magnitude of downregulation in all cell lines. However, Nestin was slightly more downregulated than βIII-tubulin in all cell lines except U87. Furthermore, downregulation of Nestin and βIII-tubulin is much stronger in LN18, U251 and A172 than in U118 and U87. Students t-test shows significant differences in expression of Nestin in LN18 (p = 0.005), U251 (p = 0.021), A172 (p = 0.008) and U118 (p = 0.006), whereas downregulation of βIII-tubulin is significant in LN18 (p = 0.007) and A172 (p = 0.008). Downregulation of βIII-tubulin was not statistically significant in U251 (p = 0.064), U118 (p = 0.135) or U87 (p = 0.656), and neither was downregulation of Nestin in U87 (p = 0.971).

5.2.2 Expression of cell line markers in hypoxia – immunocytochemistry

The half life of intermediate filaments like Nestin and GFAP is reported to be eight days[82], and microtubules are highly dynamic[83]. The time span of 4-12 days was therefore chosen, because it should be adequate to detect differences in protein expression. Cells were also cultured in hypoxia at 0.5 % oxygen for five weeks to see the long time effect of hypoxia on the expression of cell line markers. Expression of CD133, Nestin, βIII-tubulin and GFAP on cells incubated in hypoxia at 2 % and 0.5 % oxygen and in normoxia was investigated under a fluorescent microscope. ICC data is shown for cells cultured in normoxia and for cells cultured in hypoxia at 0.5 % oxygen for eight days.

To examine the induction stemness in glioma cell lines cultured in hypoxia, expression of CD133 in the previously described panel of five glioma cell lines was investigated in hypoxia at 0.5 % oxygen and in normoxia (figure 5.2.2.1). We also included the NCH-644 (table 3.1), which is a primary glioma cell line enriched for CD133 positive cells as the positive control.
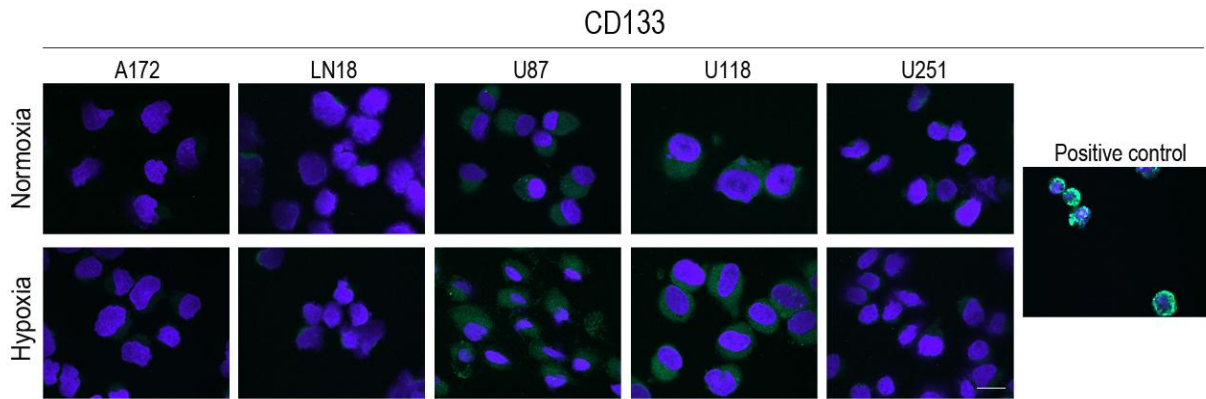
Results

Figure 5.2.2.1: Upper panels show confocal images of glioma cell lines immunostained for CD133 in cells kept in standard conditions with 21 % oxygen for a few passages. Lower panels show CD133 expression in cell lines from the same cultures after incubation in 0.5 % oxygen for eight days. Scale bars = 20 µm, nuclear counterstaining: DAPI (blue), CD133: FITC (green). CD133 expression has been compared to the positive control NCH-644 (right). NCH-644 is a non-adherent primary cell, all samples have therefore been cytospun and fixed according to chapter 4.3.2 before staining.

ICC revealed no CD133 expression neither in normoxia nor in hypoxia, which suggests that hypoxia that hypoxia does not induce stem cell like features in the five glioma cell lines investigated here (n = 2).
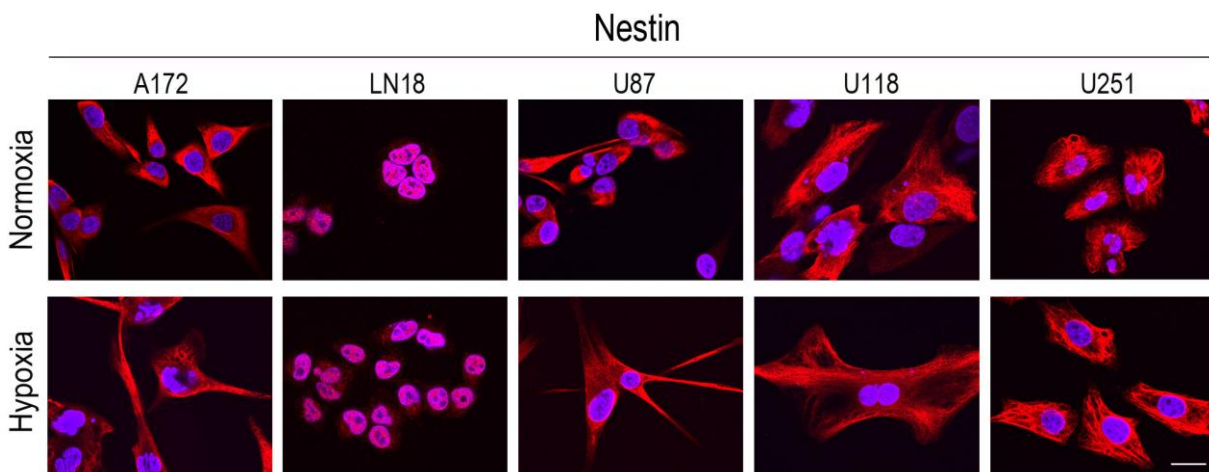

Figure 5.2.2.2: Upper panels show confocal images of glioma cells immunostained for Nestin after cultured in 21 % oxygen for a few passages. Lower panels show staining for Nestin in cell lines from the same cultures after incubation in 0.5 % oxygen for eight days. Scale bars = 20 μm, nuclear counterstaining: DAPI (blue), Nestin: Texas Red (red).

Expression of Nestin was examined by ICC after maintaining the panel of cell lines in normoxia and after incubation of the same cell lines for eight days in hypoxia at 0.5 % oxygen (figure 5.2.2.2). All cells in the three cell lines A172, U251 and LN18 are stained positive for

Nestin, regardless of oxygen concentration. Both the U87 and U118 contained a mixture of Nestin positive and negative cells, but the staining pattern did not differ between cells cultured in normoxia vs. hypoxia. LN18 seemed to have a more nuclear distribution of the protein, while the other cell lines solely showed cytoplasmic staining (n=2).
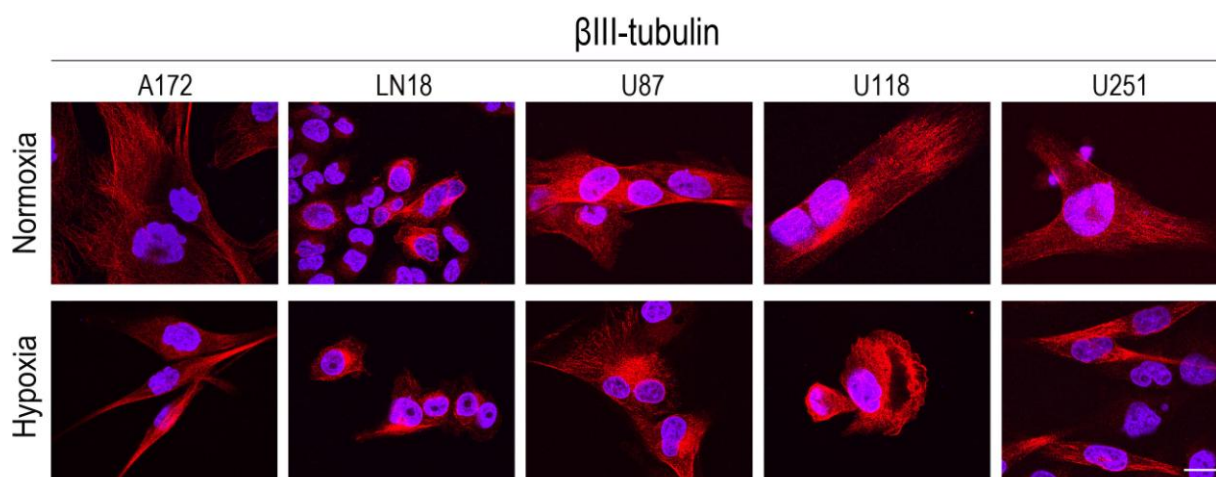

Figure 5.2.2.3: Upper panels show confocal images of immunostaining for βIII-tubulin in cells cultured in 21 % oxygen for a few passages. Lower panels show immunostaining of βIII-tubulin in cell lines from the same cultures after incubation in 0.5 % oxygen for eight days. Scale bars = 20 µm, nuclear counterstaining: DAPI (blue), βIII-tubulin: Texas Red (red).

βIII-tubulin is the isoform of the microtubule β-subunit mainly found in neurons, and is therefore commonly used as a neuronal marker. Expression of βIII-tubulin was examined by ICC after maintaining the panel of cell lines in normoxia and after incubation for eight days in hypoxia at 0.5 % oxygen (figure 5.2.2.3). Expression of βIII-tubulin was seen in all cell lines with no clear difference between the two conditions. All cell lines showed both positively and negatively stained cells, with positive cells showing a filamentous distribution of the protein. In some cells filaments spread throughout the cytoplasm from a nucleation center in proximity to the nucleus. In other cells the βIII-tubulin network seemed to be more unorganized. Also, structures resembling the mitotic spindle were positively stained in dividing cells (n = 2).
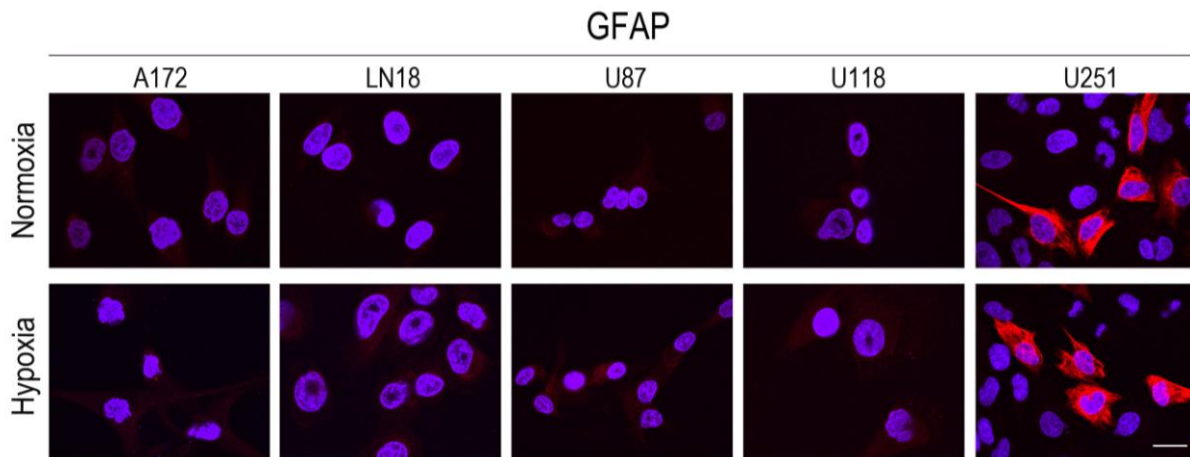
Figure 5.2.2.4: Upper panels show confocal imaging of glioma cells lines immunostained for GFAP after culturing in 21 % oxygen. Lower panels show staining for GFAP in cell lines from the same cultures after incubation in 0.5 % oxygen for eight days. Scale bars = 20 µm, nuclear counterstaining: DAPI (blue), GFAP: Texas Red (red).

Only one of the cell lines in our panel, U251, was positive for GFAP (figure 5.2.2.4). This was seen both in cells cultured in normoxia and in cells incubated in hypoxia at 0.5 % for eight days. The positive cells of U251 are seen as small clusters that stained positive for GFAP. The other cell lines were negative for GFAP both when maintained in normoxia and after incubation in hypoxia for eight days (n = 2).

Overall, when cell line markers were investigated by ICC, there was no marked difference between cells cultured under normoxia or hypoxia. We also assessed expression in glioma cells cultured in 2 % oxygen and at day four, twelve and after five weeks but found no consistent changes (data not shown). This applied to all four cell line markers and in all five cell lines investigated.

5.3 Cell proliferation, cell death and cell migration of glioma cell lines

5.3.1 Growth curves for three glioma cell lines in normoxia and hypoxia

To investigate the proliferation of cells incubated in hypoxia at 0.5 % oxygen compared to normoxia, growth curves were made for the cell lines LN18, U87 and U251. 10.000 cells were seeded in each of six cell flasks on day 0, three flasks were incubated in normoxia and

three in hypoxia at 0.5 % oxygen. Counting was performed on day three, six and nine. The experiment was repeated two times for each cell line (n = 3).
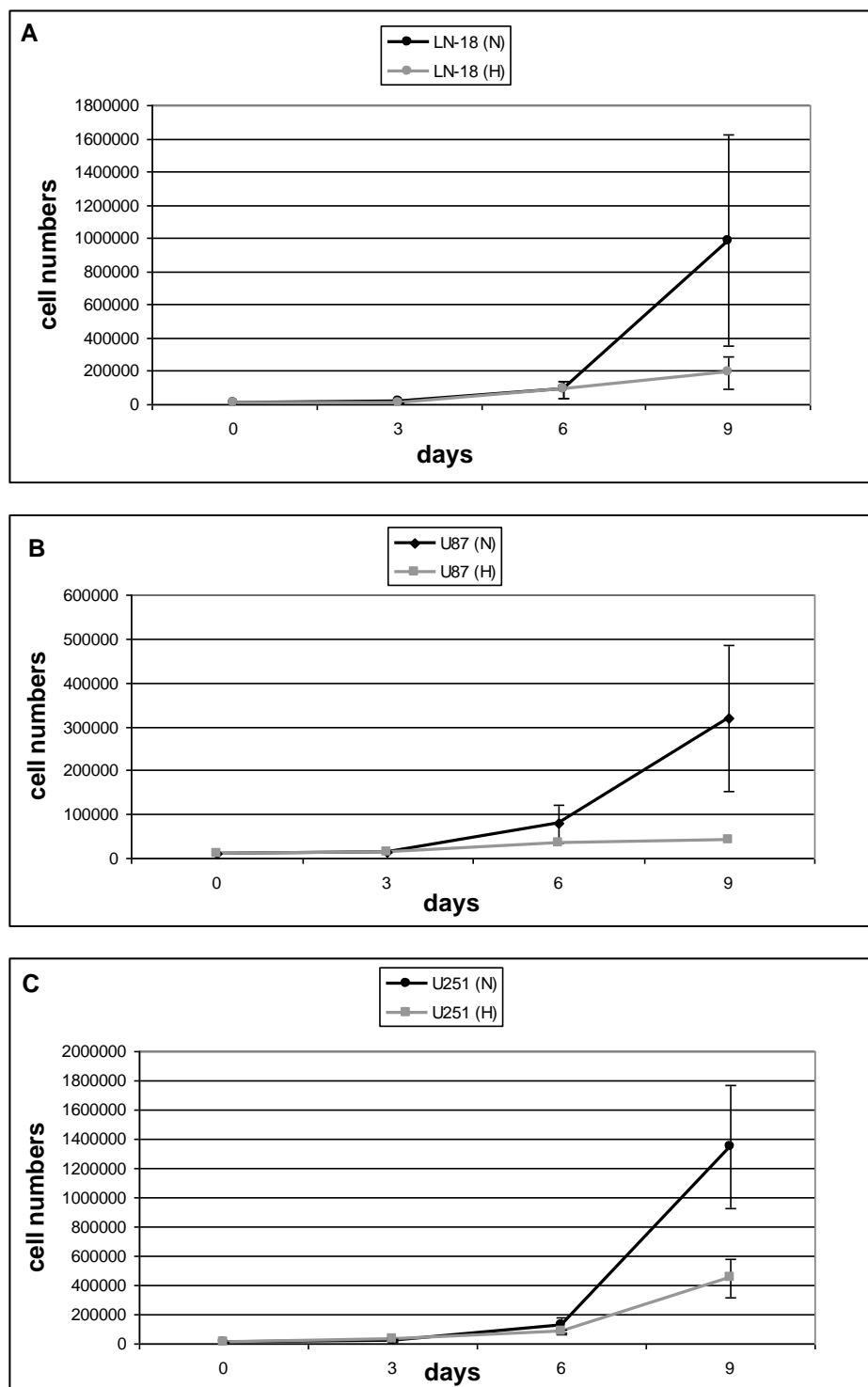

Figure 5.3.1: Growth curves for the cell lines LN18 (A), U87 (B) and U251 (C) in normoxia (N) and hypoxia (H) at 0.5 % oxygen. The x-axis indicates the days when counting was done and the y-axis indicates the number of cells that were counted in each flask. Error bars represent SEM.

It is evident from figure 5.3.1 A, B and C that cell numbers were increasing with a higher rate in normoxia, this is especially clear at day nine and the trend applies to all three cell lines. The difference in cell numbers at each time point is not statistically significant (p = 0.33, p = 0.23, p = 0.16, respectively for cell line LN18, U87 and U251 at day nine).

5.3.2 BrdU pulsing of normoxic and hypoxic cells

BrdU is a thymidine analogue, and is therefore incorporated into DNA during the S-phase of the cell cycle. By pulsing cells with BrdU for a short time (45 minutes) before fixation, and then perform ICC with an antibody directed against BrdU, we could identify all cells that had been in the S-phase in the period before fixation. BrdU pulsing was done in order to investigate the number of cells going through the S-phase at each time point when cultured in normoxia and incubated in hypoxia (figure 5.3.2). Hypoxia reduced the percentage of BrdU-positive cells (25.5 %) compared to normoxia (38.2 %, p = 0,025, n = 2).
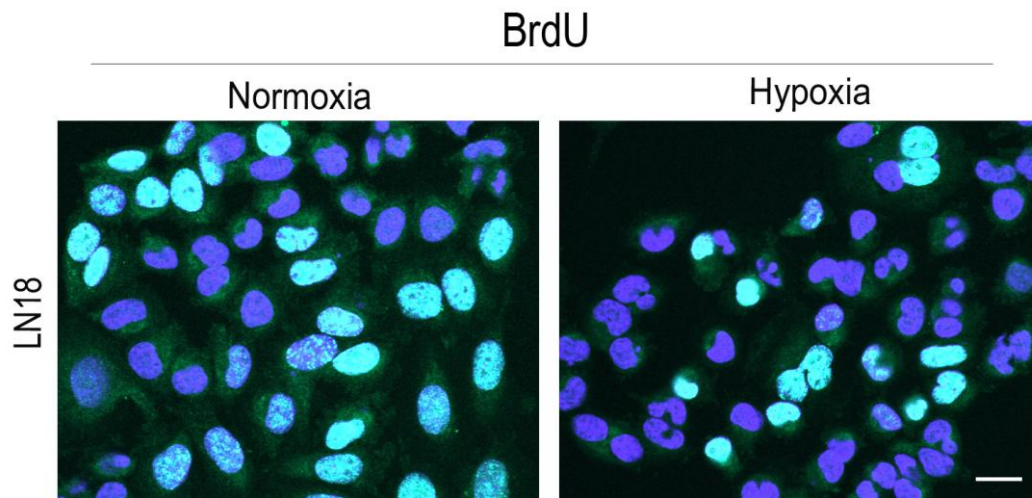
Figure 5.3.2: Confocal images of immunostaining for BrdU in the cell line LN18 cultured for a few passages in normoxia (left panel), and after culturing in hypoxia at 0.5 % oxygen for nine days (right panel). The number of green nuclei, indicating BrdU incorporation, was counted under the microscope and the BrdU-positive nuclei were displayed as a percentage of the total number of nuclei stained. Scale bars = 20 nm, nuclear counterstaining: DAPI (blue), BrdU: FITC (green).

5.3.3 Flow cytometric DNA analysis of normoxic and hypoxic cells

Cell cycle distribution was analyzed in the cell line LN18 after incubation in normoxia and in hypoxia at 0.5 % oxygen for three days (n = 2).

Figure 5.3.3: DNA analysis of the cell line LN18 incubated in normoxia (left panel) and in hypoxia (right panel) at 0.5 % ox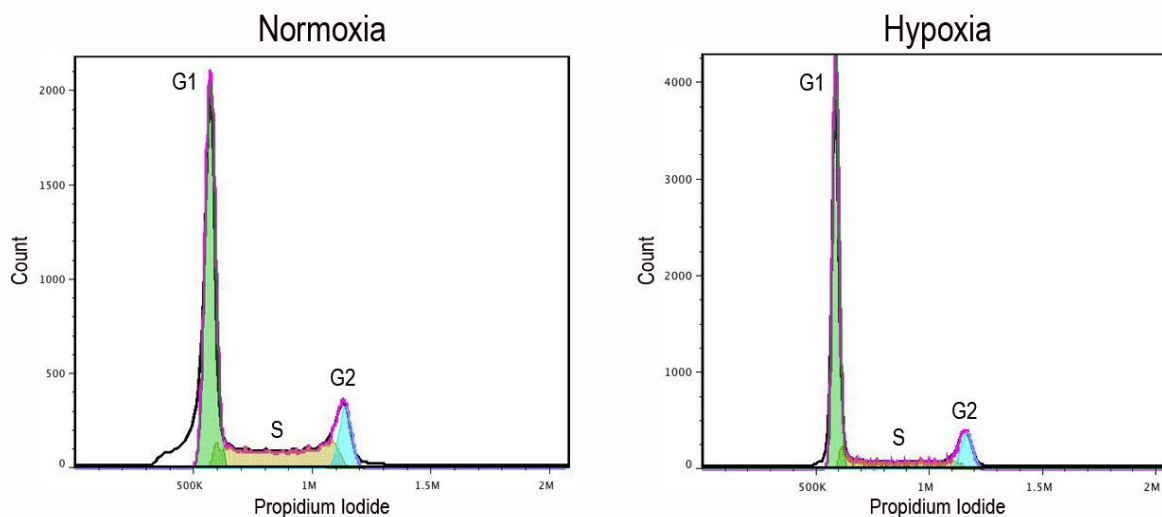ygen for three days. DNA analysis was performed after three days incubation in both oxygen conditions. Nuclei were stained with propidium iodide (PI).

Table 5.3.3: Distribution of cells in the different phases of the cell cycle when cultured in normoxia and in hypoxia at 0.5 % oxygen for three days.

Phase	Normoxia	Hypoxia
G_1	53.33 %	67.61 %
S	26.06 %	18.56 %
G_2/M	10.53 %	11.43 %

In the sample cultured in normoxia, 53.33 % of the cells were in the G_1-phase, 26.06 % were S-phase cells and 10.53 % were in the G_2/M-phase. The sample from three days incubation in hypoxia had 67.61 % G_1 cells, 18.56 % S-phase cells and 11.43 % of the cells were in the G_2/M-phase (figure and table 5.3.3). Hence there were more cells in the S-phase after three days incubation in normoxia than after three days incubation in hypoxia, confirmed by correspondingly fewer cells in the G_1 phase in normoxia than in hypoxia. No aneuploidity was detected in the samples (n = 2).

Results

5.3.4 Apoptosis assay with normoxic and hypoxic cells

We used FITC-conjugated Annexin-V, a human anticoagulant with high affinity for apoptosis-associated PS, to asses the fraction of apoptotic cells by flow cytometry. PI was used to distinguish early apoptotic cells from late apoptotic and necrotic cells (n = 2).
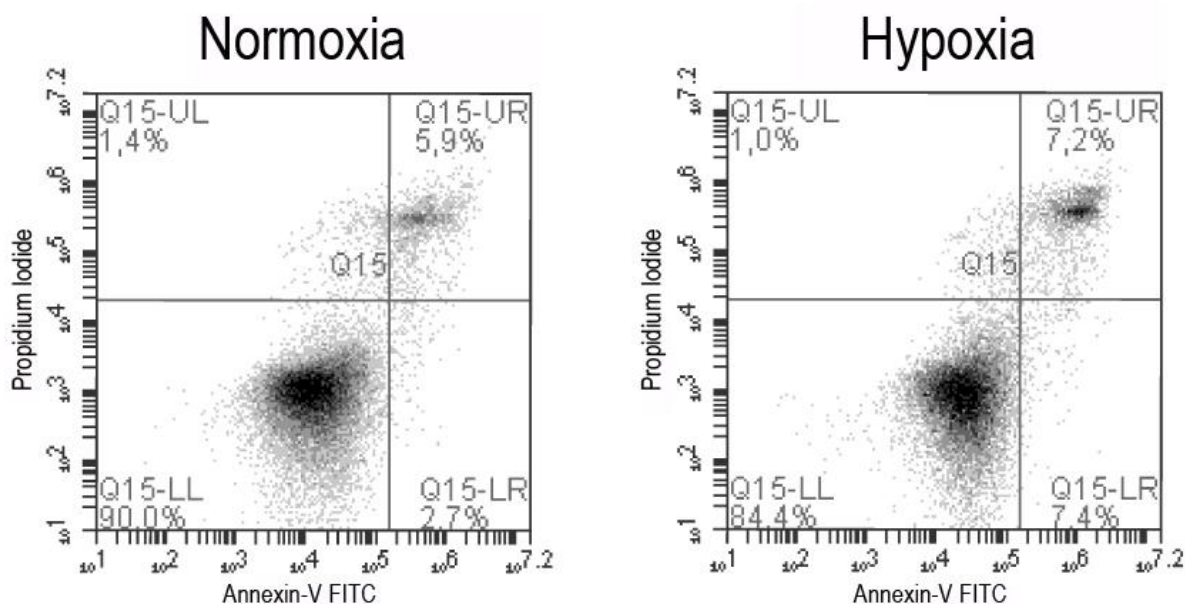

Figure 5.3.4: Dot plots representation of the LN18 cell line when cultured in normoxia (A) and after incubation in hypoxia at 0.5 % for three days (B). Viable cells stayed unstained and are seen in the lower left quadrant. FITC-conjugated Annexin-V (FL-1) was used to detect apoptotic cells, which are seen as a population in the lower right quadrant. PI (FL-3) was used to separate late apoptotic/necrotic cells, which are seen as the population in the upper right quadrant.

Table 5.3.4: The percentage of cells comprising the three different populations of live, apoptotic and late apoptotic/necrotic cells when cultured in normoxia and in hypoxia at 0.5 % oxygen for three days.

Condition	Normoxia	Hypoxia
Live	90.0 %	84.4 %
Apoptotic	2.7 %	7.4 %
Late apoptotic/necrotic	5.9 %	7.2 %

The percentage of apoptotic cells was higher after three days in hypoxia (7.4 %) than in normoxia (2.7 %, figure and table 5.3.4). Late apoptosis or necrosis was also slightly higher in hypoxia, with 7.2 % of cells compared to 5.9 % late apoptotic or necrotic cells in normoxia. The size of the viable cell populations (84.4 % in hypoxia and 90 % in normoxia) supplemented the numbers of apoptotic and necrotic cells. Furthermore, microscopy prior to

Annexin-V staining showed higher cell numbers in the normoxic compared to the hypoxic samples.

5.3.5 Glioma cell lines migrate slower when cultured in 0.5 % oxygen

Since several studies previously have shown that hypoxia may promote tumor invasion and glioma cell invasion, we wanted to study the effect of various oxygen concentrations in our panel of glioma lines. Thus, we used a wound healing assay combined with ECIS-monitoring to assess cell migration.
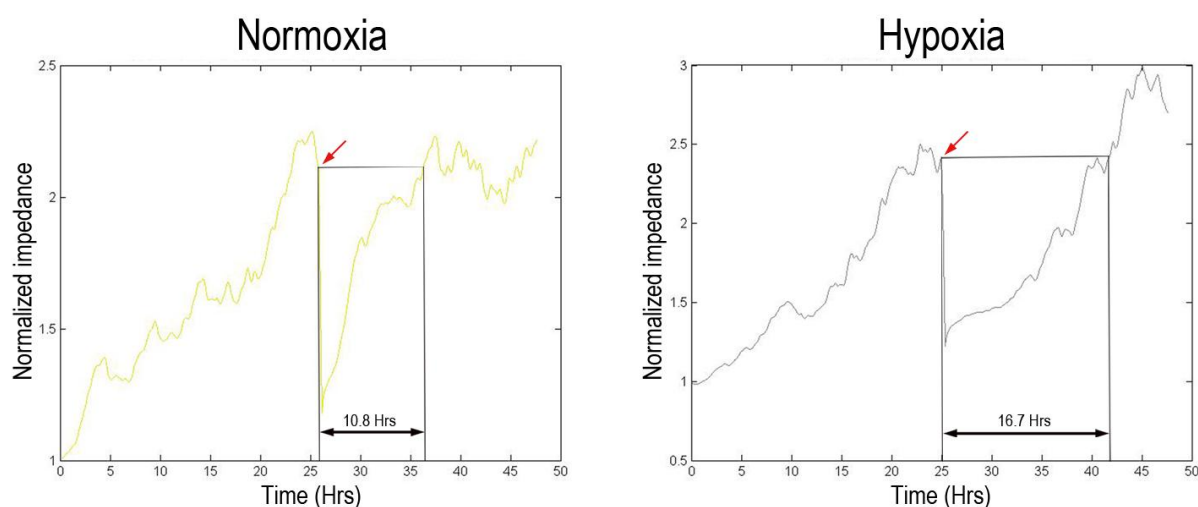
Figure 5.3.5: The ECIS graphs show wounding and subsequent migration of U251 cells cultured in normoxia (left panel) and in hypoxia at 0.5 % oxygen (right panel). The x-axis indicates hours and the y-axis the impedance. The red arrow indicates the time of wounding.

Increasing impedance at the beginning of the experiment showed a rising number of cells growing on the electrode (figure 5.3.5). When confluent, wounding/killing of the cells was performed, as seen as the sudden drop in impedance. Then the time was measured until the impedance was back at the same level as directly before wounding. The experiment was performed with the cell line U251 in normoxia (n = 5) and in hypoxia (n = 8) at 0.5 % oxygen. The average time it took for the cells to migrate back onto the electrode was measured to 9.1 hours for cells in normoxia and 15.9 hours for cells in hypoxia (p = 0.0096). Thus, cell migration properties seem to be impaired in cells cultured in hypoxia at 0.5 % when comparing to normoxic cells.

6 Discussion

Hypoxia contributes to the cellular environment both in normal development and disease, and the cellular adaption to hypoxia is accompanied by extensive changes in cell behavior. In cancer, hypoxia triggers angiogenesis, promotes tumor cell invasion and mediates resistance to both chemo- and radiotherapy. Collectively, these data suggest that hypoxia increases tumor aggressiveness and is associated with a poor prognosis.

In recent years, cancer stem cells have been isolated from various solid tumors, including glioblastoma multiforme[90, 91]. CSCs have been linked to treatment resistance similar to hypoxia. Thus, it is conceivable that the effect of hypoxia is mediated through its effects on the CSC pool. Recently, several studies have reported hypoxia-induced expression of stem cell markers together with higher clonogenic and proliferative properties and less apoptosis in hypoxia[56, 66, 88, 90]. In contrast, others has shown that proliferation cease in hypoxia[88].

Currently, both primary tumor tissue directly from the patient and in vitro propagated cancer cell lines are frequently used in experimental studies. Whereas primary tumor tissue mimics the tumor *in situ* more closely, the limited availability of such tissue has restricted their use. Moreover, the extensive cellular heterogeneity within primary tissue represents a challenge, and not all patient biopsies can be propagated *in vitro*. In contrast, experiments using cancer cell lines can be easily standardized, although their relevance to human tumors can be compromised through prolonged culturing *in vitro*[77]. However, these cell lines are in widespread use, which allows for comparison of data obtained in different labs. Thus, we investigated the response to hypoxia in a panel of five commonly used human glioma cell lines (cultured in serum containing medium) by assessing their expression of cell line markers as well as growth rates and migratory capacity in normoxia and hypoxia.

6.1 Response to hypoxia

6.1.1 HIF-1α is stabilized and translocated in hypoxia conditioned glioma cell lines

We confirmed stabilization and nuclear translocation of HIF-1α after incubation in hypoxia at 0.5 % for 24 hours. This was as expected since HIF-1α is known to become rapidly degraded under normoxic conditions, while the lack of oxygen inhibits its breakdown[25]. Additionally, cells incubated in hypoxia at 2 % oxygen showed staining for HIF-1α, albeit slightly weaker. Thus, it is apparent that there is a response to hypoxia in the cells, both in 2 % and 0.5 % oxygen, and that the effect of oxygen levels on the nuclear abundance of HIF-1α is dependent on the degree of hypoxia.

HIF-1α was investigated after five weeks incubation in hypoxia at 0.5 % as well as after 24 hours. After five weeks HIF-1α was not detectable any longer. As Nordgren and Tavassoli reviews, one of the HIF-3α isoforms, inhibitory PAS domain protein (IPAS) seems to be a downstream target of HIF-1α. Thus IPAS is upregulated in hypoxia creating a negative feedback loop for regulation of HIF-1α. This is proposed to provide the cell with a defense mechanism against activation of HIF-1α for a prolonged time[76], and might explain the absence of HIF-1α after five weeks seen in our experiments. Also, there is a possibility that other transcription factors take over the function of HIF-1α during prolonged hypoxia. For example, Seidel *et al* demonstrated that HIF-2α was upregulated upon HIF-1α knockdown in a primary GBM cell line cultured at 1 % oxygen[66]. It is therefore possible that downregulation of HIF-1α during prolonged hypoxia was accompanied by upregulation of HIF-2α in our experiments as well. Other groups report normoxic HIF-1α activity in cell lines such as U87[92], which we could not detect in the present study. This may be due to the fact that many different studies are performed on variants of the commercial cell lines available today. These variants have arisen as many cell lines have been cultured extensively in different labs for several decades.

One could observe variations between the five cell lines in the panel concerning protein levels of hypoxia-induced HIF-1α. These cell lines were initially isolated from different glioblastomas which are tumors that display high levels heterogeneity. Internal differences among these cell lines might therefore reflect this heterogeneity in the original tumor, further exemplified by their diversity regarding traits such as morphology and proliferation rates *in*

vitro. Notably, such variations in HIF-1α levels are also seen when primary cell lines established from different GBM patients are cultured in 1 % oxygen[85]. If similar variations occur in GBMs *in situ*, this may be one factor underlying the variable response to radiation treatment among GBM patients.

6.1.2 Glioma cell lines express CAIX to varying extent when cultured in hypoxia

Although CAIX was uniformly upregulated in response to hypoxia, changes in expression levels were not significant for any of the cell lines. CAIX expression levels increased markedly in the cell lines A172, U118 and U251, whereas LN18 and U87 showed a smaller upregulation in CAIX expression. In addition to a high degree of variance between the three samples of RNA isolated, the lack of induced CAIX expression might be due to several other factors. One possible explanation is that HIF-1α is the only transcription factor known to regulate CAIX[76], and HIF-2α is proposed to replace HIF-1α as the active hypoxia inducible factor during prolonged (> 72 hrs) hypoxia[93]. Relatively low levels of CAIX in two cell lines after eight days incubation in hypoxia at 0.5 % oxygen might therefore be explained by absent HIF-1α in the nucleus. These findings are in agreement with the lack of HIF-1α after four weeks incubation in hypoxia at 0.5 % oxygen. Additionally, Said *et al* (2008) also reported that CAIX is differentially induced by hypoxia in four different glioma cell lines[92].

6.2 Expression of cell line markers in hypoxia

6.2.1 Expression of the stem cell markers CD133 and Nestin is not increased in hypoxia conditioned glioma cell lines

The surface protein CD133 has long been considered as the principal stem cell marker, and is expressed in precursor cells of many tissues in the body as well as in different cancer types[84]. Several studies recent years also report an upregulation of CD133 in glioma cells derived from patients when cultured in hypoxia, suggesting that hypoxia induces stemness[85]. Nestin is an intermediate filament expressed in neural stem cells during development and is later replaced by GFAP in mature astrocytes and with neurofilaments in neurons. Nestin is also found to be re-expressed in reactive astrocytes and connected to re-entry into the cell cycle.

Therefore, Nestin is similar to CD133, associated with immatureness and stem cell features[86]. We therefore investigated these two stem cell markers to asses whether hypoxia could induce stemness in glioma cell lines.

None of the investigated glioma cell lines did reveal any expression of CD133 neither when cultured in normoxia nor when incubated for eight days at 0.5 % oxygen. This contradict to some extent previous studies done on biopsy material[85, 88, 90] and on some of the same glioma cell lines as in our panel[88, 95]. These studies report increased expression of such stem cell markers such as CD133 and Nestin under hypoxia. However these experiments were carried out using serum-free medium which reportedly favors the expansion of stem cell like cells. Our cell lines have been adapted to serum-containing medium through numerous passages according to the commercial provider ATTC. Thus we chose to keep culture conditions constant to allow for comparisons with data on these cell lines published by other groups. In addition we have previously shown that several of these cell lines did not express CD133 when cultured in stem cell medium[96]. However, even if some glioma cell lines have the ability to re-express CD133, we can conclude that hypoxia is not enough for induction of CD133 expression in serum-containing medium.

All five cell lines in the panel used in this study display clear expression of Nestin also in hypoxia, although qRT-PCR shows a downregulation of mRNA synthesis compared to normoxic levels. LN18 is the only cell line with clear nuclear staining of Nestin. The same phenomenon has been reported by other groups[97], although the function of Nestin in the nucleus is not known. Glial tumors and glioma cell lines are known to express Nestin. Moreover, contrary to our findings Kolenda *et al* has shown that Nestin is upregulated in hypoxia in the cell line U87, although they also report expression in normoxia[88]. Notably, the study of Kolenda *et al* was also performed in serum free medium. Instead, downregulation of Nestin in our experiments emphasized the trend observed also in our functional studies, suggesting an overall slowdown of cellular processes under hypoxia. As such, these findings do not point to any dedifferentiation of glioma cell lines in hypoxia, like others have reported[56, 66, 88, 90].

6.2.2 Glioma cell lines downregulate cell lineage markers βIII-tubulin and GFAP in hypoxia

ICC did not reveal any clear differences in expressions of βIII-tubulin or GFAP when comparing cells maintained in normoxic conditions and in hypoxia at 0.5 % oxygen for eight days. However, qRT-PCR demonstrated a downregulation of these markers in hypoxia.

βIII-tubulin is primarily used as a neuronal marker, and is not normally expressed in astrocytes[87]. (Therefore, Katsetos *et al* (2001) proposed that βIII-tubulin expression in astrocytic tumors to be a marker of less differentiated, highly proliferative cells associated with high tumor grade[87]. Particularly, Katsetos *et al* found βIII-tubulin positive cells in astrocytomas to be co-localized with strong staining of the proliferation marker Ki-67[87]. Expression of βIII-tubulin in GBMs and other astrocytomas is therefore a trait of transformed cells and may represent dedifferentiation, which is associated with CSCs. Moreover, Katsetos *et al* (2009) report increased expression of βIII-tubulin in the areas adjacent to pseudopalisading necrosis in GBMs[83], connecting βIII-tubulin to hypoxia. They postulate that βIII-tubulin is implicated in adaptation to oxidative stress and glucose deprivation, a hallmark of the hypoxic environment.) The downregulation of βIII-tubulin in hypoxia which was seen in our experiment does not support this hypothesis.

GFAP is an intermediate filament expressed in mature astrocytes[88]. U251 was the only cell line expressing GFAP, and in this cell line only small cell clusters were positive. It has previously been documented that GFAP becomes downregulated in conventional GBM cell lines and in glioblastoma biopsies cultured over time[89], and the low expression of GFAP is therefore expected. As for the other cell line markers, expression of GFAP in U251 was downregulated in hypoxia.

In addition, there was a considerable variation between the different cell lines in the magnitude with which the different cell line markers were downregulated under hypoxia. Like for HIF-1α and CAIX expression, this may arise because these cell lines are isolated from different tumors.

Furthermore, it is known that under hypoxic conditions, cells decrease their overall RNA synthesis by 50-70 %[31]. Accordingly, the observed decline in expression of cell line markers

likely results from a general reduction in RNA synthesis. Especially this would seem reasonable for proteins that are not vital to cell survival, but whose expression may result from deregulated gene expression in cancer cells. An overall downregulation of the cellular machinery is also in correspondence with the other findings in our work; less proliferation and slower migration.

6.3 Proliferation and apoptosis in hypoxia conditioned glioma cell lines

6.3.1 Proliferation of glioma cell lines cease in hypoxia

All cell lines examined uniformly displayed reduced growth rates in hypoxia at 0.5 % oxygen. Still, at each time point there is a high standard error of the mean for the three repeats in the experiment, which can explain why these findings were not significant. This variation may be due to an inaccuracy in the counting and seeding methods that may result in initial cell numbers deviating from 10,000. Even though there was a great variation between each repetition, each repeat itself clearly displayed the same biological trend with fewer cells at day nine in hypoxia than in normoxia. This is further underlined by examination of BrdU incorporation and DNA analysis of LN18 cells maintained in normoxia and LN18 cells incubated in hypoxia at 0.5 % oxygen. The number of BrdU positive cells was significantly higher in normoxia than after nine days in hypoxia, demonstrating more proliferating cells in normoxia. Also, the DNA analysis revealed elevated S-phase cell numbers in normoxia compared to cells incubated for three days in hypoxia. This is in agreement with previous findings that hypoxia induces arrest in the G_1-phase of the cell cycle, both in a HIF-1α dependent and independent manner[98, 99].

As mentioned above, Nestin and βIII-tubulin are associated with the ability of rapid proliferation. Downregulation of these two markers in hypoxia could therefore mirror the cease in proliferation that we see from the growth curves. Kolenda *et al* (2010) shows the same trend; spheroid size and number as well as Ki-67 staining were negatively influenced by hypoxia compared to normoxia. On the other hand they found an upregulation of stem cell markers in hypoxia, contradictory to what we found[56, 88]. While some groups report inhibited growth in hypoxia[88, 100], there are others that report that hypoxia promotes better growth with

Discussion

higher sphere forming abilities[85]. Notably, these experiments were performed in serum free medium.

6.3.2 Hypoxia induces apoptosis in glioma cell lines

Flow cytometry showed a moderately but significantly increased percentage of apoptotic and late apoptotic/necrotic cells after incubating LN18 in hypoxia at 0.5 % oxygen for three days, compared to normoxia. Furthermore, FCM revealed an accumulation in the G_1-phase, probably due to G_0/G_1 check point activation. Schmaltz *et al* (1998) reported that when transformed rat embryo fibroblasts were grown in hypoxia, apoptosis was not triggered unless the cultures experienced acidosis. Also, non-transformed cells were arrested in a G_0/G_1 check point in hypoxia[24]. Since our glioma cell culture experienced G_1-arrest under hypoxia, the resulting cell numbers may have been too low to create an acidic environment despite hypoxia-induced glycolysis. Accordingly, this may have had a protective effect against apoptosis. In contrast to what we see, Schmaltz *et al* report overriding of the G_0/G_1 check point of transformed cells in non-acidic hypoxia, followed by higher proliferative abilities of cells in hypoxia than in normoxia[24]. However, different cell types were used in these studies, and may explain discrepancies between their and our findings.

6.4 Migratory abilities of hypoxia conditioned glioma cell lines are impaired in hypoxia

Wound healing performed in normoxia and hypoxia showed that cells migrate back into the wounded area faster in standard conditions than when the same experiment is done in hypoxia at 0.5 % oxygen. Contrary to this, several findings report an increased ability to migrate under hypoxic conditions, as described by Zagzag *et al.* Zagzag showed that two glioma cell lines increase migration when cultured in 1% oxygen. Several mechanisms such as downregulation of E- and N-cadherins in hypoxia[100], increased signaling through the Akt pathway[101], and upregulation of the chemokine receptor CXCR4 by HIF-1α[102] have been proposed to increased migration and invasion. Taken together, the findings that cells migrate slower are therefore contrary to expectations. However, impaired migratory abilities may reflect the general slow down in cellular processes seen by cell cycle arrest and downregulation of gene transcription. The use of biopsy material and/or serum free medium in other studies might contribute to the diverging results between those and the present investigation.

6.5 Conclusion

In this work, we investigated the impact of hypoxia on the expression of cell line markers and cell behavior in a panel of human glioma cell lines.

We demonstrated stabilization of the transcription factor HIF-1a and induction of its downstream target CAIX, confirming that our model sufficiently mimicked the hypoxic niche in tumors *in situ*.

Nestin and βIII-tubulin were both extensively expressed in all glioma cell lines tested. GFAP was only expressed in a minor part of U251 cells and CD133 was not expressed in any of the cell lines neither in normoxia nor hypoxia. All markers that were expressed in standard tissue culture conditions at 21 % oxygen were also expressed after up to five weeks in hypoxia at 0.5 %, although they were all downregulated as assessed by q-RT-PCR.

Growth curves, BrdU labeling and FCM all showed decreased growth under hypoxia. Furthermore, FCM demonstrated that hypoxia was associated with an accumulation of cells in the G1 phase and more cells undergoing apoptosis under hypoxia.

In addition, ECIS experiments showed slower glioma cell migration in hypoxia compared to normoxia.

Based on the above findings, we conclude that a stem like phenotype is not induced in hypoxia conditioned glioma cell lines. Furthermore, these findings are at odds with what have previously been reported by other groups.

7. Future perspectives

Several studies, including our work, have presented conflicting results regarding the effect of hypoxia on stem like properties in brain tumors. I therefore believe that future studies should address these controversies. The present study was conducted on conventional glioma cell lines cultured in serum-containing medium. Studies addressing stemness in CNS-tumors have generally been performed in serum-free medium, the type of medium reportedly maintaining stem cells. Moreover, in each study only a few specimens from surgical resections have been examined. This study should therefore be expanded to include parallel experiments on conventional glioma cell lines in serum-free medium. Additionally, the study should comprise experiments performed on a larger selection of biopsy material derived from GBM patients to evaluate the effect of hypoxia on the expression of stem cell markers and cell behavior.

Furthermore, little is known about the effect of hypoxia on the tumor stroma. However, it has become increasingly clear that tumor-stroma interactions play a major role in malignant disease. Future studies should therefore also characterize how the stromal cell compartment in tumors is affected by hypoxia.

Our lab has recently established a DsRed-expressing NOD/Scid mouse in which human tumors can be xenografted. The resulting tumors contain human tumor cells embedded in red fluorescent stromal mouse cells, which allows for fluorescence-based separation of the tumor and stromal cell compartments. Therefore, these animal models may be a valuable tool for investigating the effect of hypoxia on the tumor stroma.

References

1.   WHO: Cancer Fact sheet Number 297. Edited by 2009, p.
2.   Hanahan D, Weinberg RA: The hallmarks of cancer, Cell 2000, 100:57-70
3.   Hanahan D, Weinberg RA: Hallmarks of cancer: the next generation, Cell 2011, 144:646-674
4.   Nowell PC: The clonal evolution of tumor cell populations, Science 1976, 194:23-28
5.   Pecorino L: Molecular Biology of Cancer - Mechanisms, Targets and Therapeutics. Edited by New York, Oxford University Press Inc. , 2008,
6.   Muller PA, Vousden KH, Norman JC: p53 and its mutants in tumor cell migration and invasion, J Cell Biol 2011, 192:209-218
7.   Folkman J: Proceedings: Tumor angiogenesis factor, Cancer Res 1974, 34:2109-2113
8.   Ferrara N, Gerber HP, LeCouter J: The biology of VEGF and its receptors, Nat Med 2003, 9:669-676
9.   Steeg PS: Tumor metastasis: mechanistic insights and clinical challenges, Nat Med 2006, 12:895-904
10.   Ribatti D, Mangialardi G, Vacca A: Stephen Paget and the 'seed and soil' theory of metastatic dissemination, Clin Exp Med 2006, 6:145-149
11.   Louis DN, Ohgaki H, Wiestler OD, Cavenee WK, Burger PC, Jouvet A, Scheithauer BW, Kleihues P: The 2007 WHO classification of tumours of the central nervous system, Acta Neuropathol 2007, 114:97-109
12.   U.S. Department of Health and Human Services CfDCaPaNCI: United States Cancer Statistics: 1999–2007 Incidence and Mortality. Edited by 2010, p.
13.   Stupp R, Mason WP, van den Bent MJ, Weller M, Fisher B, Taphoorn MJ, Belanger K, Brandes AA, Marosi C, Bogdahn U, Curschmann J, Janzer RC, Ludwin SK, Gorlia T, Allgeier A, Lacombe D, Cairncross JG, Eisenhauer E, Mirimanoff RO: Radiotherapy plus concomitant and adjuvant temozolomide for glioblastoma, N Engl J Med 2005, 352:987-996
14.   Robertson LB, Armstrong GN, Olver BD, Lloyd AL, Shete S, Lau C, Claus EB, Barnholtz-Sloan J, Lai R, Il'yasova D, Schildkraut J, Bernstein JL, Olson SH, Jenkins RB, Yang P, Rynearson AL, Wrensch M, McCoy L, Wienkce JK, McCarthy B, Davis F, Vick NA, Johansen C, Bodtcher H, Sadetzki S, Bruchim RB, Yechezkel GH, Andersson U, Melin BS, Bondy ML, Houlston RS: Survey of familial glioma and role of germline p16INK4A/p14ARF and p53 mutation, Fam Cancer 2010, 9:413-421
15.   Adamson C, Kanu OO, Mehta AI, Di C, Lin N, Mattox AK, Bigner DD: Glioblastoma multiforme: a review of where we have been and where we are going, Expert Opin Investig Drugs 2009, 18:1061-1083
16.   Comprehensive genomic characterization defines human glioblastoma genes and core pathways, Nature 2008, 455:1061-1068
17.   Tysnes BB, Mahesparan R: Biological mechanisms of glioma invasion and potential therapeutic targets, J Neurooncol 2001, 53:129-147
18.   Ohgaki H, Kleihues P: Genetic pathways to primary and secondary glioblastoma, Am J Pathol 2007, 170:1445-1453
19.   Erecinska M, Silver IA: Tissue oxygen tension and brain sensitivity to hypoxia, Respir Physiol 2001, 128:263-276
20.   Csete M: Oxygen in the cultivation of stem cells, Ann N Y Acad Sci 2005, 1049:1-8
21.   Bar EE: Glioblastoma, cancer stem cells and hypoxia, Brain Pathol 2011, 21:119-129
22.   Hampton-Smith RJ, Peet DJ: From polyps to people: a highly familiar response to hypoxia, Ann N Y Acad Sci 2009, 1177:19-29

References

23.   Weir L, Robertson D, Leigh IM, Vass JK, Panteleyev AA: Hypoxia-mediated control of HIF/ARNT machinery in epidermal keratinocytes, Biochim Biophys Acta 2011, 1813:60-72

24.   Schmaltz C, Hardenbergh PH, Wells A, Fisher DE: Regulation of proliferation-survival decisions during tumor cell hypoxia, Mol Cell Biol 1998, 18:2845-2854

25.   Brahimi-Horn MC, Pouysségur J: HIF at a glance, J Cell Sci 2009, 122:1055-1057

26.   Wang GL, Jiang BH, Rue EA, Semenza GL: Hypoxia-inducible factor 1 is a basic-helix-loop-helix-PAS heterodimer regulated by cellular O2 tension, Proc Natl Acad Sci U S A 1995, 92:5510-5514

27.   Wang GL, Semenza GL: Purification and characterization of hypoxia-inducible factor 1, J Biol Chem 1995, 270:1230-1237

28.   Hankinson O: Why does ARNT2 behave differently from ARNT?, Toxicol Sci 2008, 103:1-3

29.   Semenza GL: Targeting HIF-1 for cancer therapy, Nat Rev Cancer 2003, 3:721-732

30.   Iyer NV, Kotch LE, Agani F, Leung SW, Laughner E, Wenger RH, Gassmann M, Gearhart JD, Lawler AM, Yu AY, Semenza GL: Cellular and developmental control of O2 homeostasis by hypoxia-inducible factor 1 alpha, Genes Dev 1998, 12:149-162

31.   Fandrey J: Hypoxia-inducible gene expression, Respir Physiol 1995, 101:1-10

32.   Jelkmann W: Regulation of erythropoietin production, J Physiol 2011, 589:1251-1258

33.   Loike JD, Cao L, Brett J, Ogawa S, Silverstein SC, Stern D: Hypoxia induces glucose transporter expression in endothelial cells, Am J Physiol 1992, 263:C326-333

34.   Semenza GL, Roth PH, Fang HM, Wang GL: Transcriptional regulation of genes encoding glycolytic enzymes by hypoxia-inducible factor 1, J Biol Chem 1994, 269:23757-23763

35.   Shweiki D, Itin A, Soffer D, Keshet E: Vascular endothelial growth factor induced by hypoxia may mediate hypoxia-initiated angiogenesis, Nature 1992, 359:843-845

36.   Brown JM, Giaccia AJ: The unique physiology of solid tumors: opportunities (and problems) for cancer therapy, Cancer Res 1998, 58:1408-1416

37.   Secomb TW, Hsu R, Dewhirst MW, Klitzman B, Gross JF: Analysis of oxygen transport to tumor tissue by microvascular networks, Int J Radiat Oncol Biol Phys 1993, 25:481-489

38.   Graeber TG, Osmanian C, Jacks T, Housman DE, Koch CJ, Lowe SW, Giaccia AJ: Hypoxia-mediated selection of cells with diminished apoptotic potential in solid tumours, Nature 1996, 379:88-91

39.   Semenza GL: HIF-1: mediator of physiological and pathophysiological responses to hypoxia, J Appl Physiol 2000, 88:1474-1480

40.   Gray LH, Conger AD, Ebert M, Hornsey S, Scott OC: The concentration of oxygen dissolved in tissues at the time of irradiation as a factor in radiotherapy, Br J Radiol 1953, 26:638-648

41.   De Ridder M, Verellen D, Verovski V, Storme G: Hypoxic tumor cell radiosensitization through nitric oxide, Nitric Oxide 2008, 19:164-169

42.   Zhang XP, Liu F, Wang W: Two-phase dynamics of p53 in the DNA damage response, Proc Natl Acad Sci U S A 2011,

43.   Chung WJ, Lyons SA, Nelson GM, Hamza H, Gladson CL, Gillespie GY, Sontheimer H: Inhibition of cystine uptake disrupts the growth of primary brain tumors, J Neurosci 2005, 25:7101-7110

44.   Schwartz DL, Bankson J, Bidaut L, He Y, Williams R, Lemos R, Thitai AK, Oh J, Volgin A, Soghomonyan S, Yeh HH, Nishii R, Mukhopadhay U, Alauddin M, Mushkudiani I, Kuno N, Krishnan S, Bornman W, Lai SY, Powis G, Hazle J, Gelovani J: HIF-1-

Dependent Stromal Adaptation to Ischemia Mediates In Vivo Tumor Radiation Resistance, Mol Cancer Res 2011, 9:259-270

45.   Comerford KM, Wallace TJ, Karhausen J, Louis NA, Montalto MC, Colgan SP: Hypoxia-inducible factor-1-dependent regulation of the multidrug resistance (MDR1) gene, Cancer Res 2002, 62:3387-3394

46.   Fardel O, Lecureur V, Guillouzo A: The P-glycoprotein multidrug transporter, Gen Pharmacol 1996, 27:1283-1291

47.   Rong Y, Durden DL, Van Meir EG, Brat DJ: 'Pseudopalisading' necrosis in glioblastoma: a familiar morphologic feature that links vascular pathology, hypoxia, and angiogenesis, J Neuropathol Exp Neurol 2006, 65:529-539

48.   Brat DJ, Castellano-Sanchez AA, Hunter SB, Pecot M, Cohen C, Hammond EH, Devi SN, Kaur B, Van Meir EG: Pseudopalisades in glioblastoma are hypoxic, express extracellular matrix proteases, and are formed by an actively migrating cell population, Cancer Res 2004, 64:920-927

49.   Ben-Yosef Y, Lahat N, Shapiro S, Bitterman H, Miller A: Regulation of endothelial matrix metalloproteinase-2 by hypoxia/reoxygenation, Circ Res 2002, 90:784-791

50.   Pennacchietti S, Michieli P, Galluzzo M, Mazzone M, Giordano S, Comoglio PM: Hypoxia promotes invasive growth by transcriptional activation of the met protooncogene, Cancer Cell 2003, 3:347-361

51.   Brat DJ, Van Meir EG: Vaso-occlusive and prothrombotic mechanisms associated with tumor hypoxia, necrosis, and accelerated growth in glioblastoma, Lab Invest 2004, 84:397-405

52.   Rong Y, Post DE, Pieper RO, Durden DL, Van Meir EG, Brat DJ: PTEN and hypoxia regulate tissue factor expression and plasma coagulation by glioblastoma, Cancer Res 2005, 65:1406-1413

53.   Yan SF, Mackman N, Kisiel W, Stern DM, Pinsky DJ: Hypoxia/Hypoxemia-Induced activation of the procoagulant pathways and the pathogenesis of ischemia-associated thrombosis, Arterioscler Thromb Vasc Biol 1999, 19:2029-2035

54.   Sciacca FL, Ciusani E, Silvani A, Corsini E, Frigerio S, Pogliani S, Parati E, Croci D, Boiardi A, Salmaggi A: Genetic and plasma markers of venous thromboembolism in patients with high grade glioma, Clin Cancer Res 2004, 10:1312-1317

55.   Reya T, Morrison SJ, Clarke MF, Weissman IL: Stem cells, cancer, and cancer stem cells, Nature 2001, 414:105-111

56.   Heddleston JM, Li Z, McLendon RE, Hjelmeland AB, Rich JN: The hypoxic microenvironment maintains glioblastoma stem cells and promotes reprogramming towards a cancer stem cell phenotype, Cell Cycle 2009, 8:3274-3284

57.   Zhou S, Schuetz JD, Bunting KD, Colapietro AM, Sampath J, Morris JJ, Lagutina I, Grosveld GC, Osawa M, Nakauchi H, Sorrentino BP: The ABC transporter Bcrp1/ABCG2 is expressed in a wide variety of stem cells and is a molecular determinant of the side-population phenotype, Nat Med 2001, 7:1028-1034

58.   Doyle LA, Yang W, Abruzzo LV, Krogmann T, Gao Y, Rishi AK, Ross DD: A multidrug resistance transporter from human MCF-7 breast cancer cells, Proc Natl Acad Sci U S A 1998, 95:15665-15670

59.   Pistollato F, Chen HL, Schwartz PH, Basso G, Panchision DM: Oxygen tension controls the expansion of human CNS precursors and the generation of astrocytes and oligodendrocytes, Mol Cell Neurosci 2007, 35:424-435

60.   Gustafsson MV, Zheng X, Pereira T, Gradin K, Jin S, Lundkvist J, Ruas JL, Poellinger L, Lendahl U, Bondesson M: Hypoxia requires notch signaling to maintain the undifferentiated cell state, Dev Cell 2005, 9:617-628

References

61.   Li Z, Bao S, Wu Q, Wang H, Eyler C, Sathornsumetee S, Shi Q, Cao Y, Lathia J, McLendon RE, Hjelmeland AB, Rich JN: Hypoxia-inducible factors regulate tumorigenic capacity of glioma stem cells, Cancer Cell 2009, 15:501-513

62.   Platet N, Liu SY, Atifi ME, Oliver L, Vallette FM, Berger F, Wion D: Influence of oxygen tension on CD133 phenotype in human glioma cell cultures, Cancer Lett 2007, 258:286-290

63.   Blazek ER, Foutch JL, Maki G: Daoy medulloblastoma cells that express CD133 are radioresistant relative to CD133- cells, and the CD133+ sector is enlarged by hypoxia, Int J Radiat Oncol Biol Phys 2007, 67:1-5

64.   Covello KL, Kehler J, Yu H, Gordan JD, Arsham AM, Hu CJ, Labosky PA, Simon MC, Keith B: HIF-2alpha regulates Oct-4: effects of hypoxia on stem cell function, embryonic development, and tumor growth, Genes Dev 2006, 20:557-570

65.   El Haddad N, Heathcote D, Moore R, Yang S, Azzi J, Mfarrej B, Atkinson M, Sayegh MH, Lee JS, Ashton-Rickardt PG, Abdi R: Mesenchymal stem cells express serine protease inhibitor to evade the host immune response, Blood 2011, 117:1176-1183

66.   Seidel S, Garvalov BK, Wirta V, von Stechow L, Schanzer A, Meletis K, Wolter M, Sommerlad D, Henze AT, Nister M, Reifenberger G, Lundeberg J, Frisen J, Acker T: A hypoxic niche regulates glioblastoma stem cells through hypoxia inducible factor 2 alpha, Brain 2010, 133:983-995

67.   Wen PY, Kesari S: Malignant gliomas in adults, N Engl J Med 2008, 359:492-507

68.   Stupp R, Tonn JC, Brada M, Pentheroudakis G: High-grade malignant glioma: ESMO Clinical Practice Guidelines for diagnosis, treatment and follow-up, Ann Oncol 2010, 21 Suppl 5:v190-193

69.   U.S Department og Health & Human Services F, U.S Food and Drug Administration: Avastin (Bevacizumab) Information. Edited by 2011, p.

70.   Zuniga RM, Torcuator R, Jain R, Anderson J, Doyle T, Schultz L, Mikkelsen T: Rebound tumour progression after the cessation of bevacizumab therapy in patients with recurrent high-grade glioma, J Neurooncol 2010, 99:237-242

71.   Keunen O, Johansson M, Oudin A, Sanzey M, Rahim SA, Fack F, Thorsen F, Taxt T, Bartos M, Jirik R, Miletic H, Wang J, Stieber D, Stuhr L, Moen I, Rygh CB, Bjerkvig R, Niclou SP: Anti-VEGF treatment reduces blood supply and increases tumor cell invasion in glioblastoma, Proc Natl Acad Sci U S A 2011, 108:3749-3754

72.   Raizer JJ, Abrey LE, Lassman AB, Chang SM, Lamborn KR, Kuhn JG, Yung WK, Gilbert MR, Aldape KA, Wen PY, Fine HA, Mehta M, Deangelis LM, Lieberman F, Cloughesy TF, Robins HI, Dancey J, Prados MD: A phase II trial of erlotinib in patients with recurrent malignant gliomas and nonprogressive glioblastoma multiforme postradiation therapy, Neuro Oncol 2010, 12:95-103

73.   Fan QW, Weiss WA: Targeting the RTK-PI3K-mTOR axis in malignant glioma: overcoming resistance, Curr Top Microbiol Immunol 2010, 347:279-296

74.   Stadler P, Becker A, Feldmann HJ, Hansgen G, Dunst J, Wurschmidt F, Molls M: Influence of the hypoxic subvolume on the survival of patients with head and neck cancer, Int J Radiat Oncol Biol Phys 1999, 44:749-754

75.   Overgaard J: Hypoxic radiosensitization: adored and ignored, J Clin Oncol 2007, 25:4066-4074

76.   Nordgren IK, Tavassoli A: Targeting tumour angiogenesis with small molecule inhibitors of hypoxia inducible factor, Chem Soc Rev 2011,

77.   Hughes P, Marshall D, Reid Y, Parkes H, Gelber C: The costs of using unauthenticated, over-passaged cell lines: how much more data do we need?, Biotechniques 2007, 43:575, 577-578, 581-572 passim

78.   Schmittgen TD, Livak KJ: Analyzing real-time PCR data by the comparative C(T) method, Nat Protoc 2008, 3:1101-1108

79.   Lal A, Peters H, St Croix B, Haroon ZA, Dewhirst MW, Strausberg RL, Kaanders JH, van der Kogel AJ, Riggins GJ: Transcriptional response to hypoxia in human tumors, J Natl Cancer Inst 2001, 93:1337-1343

80.   Dewhirst MW, Ong ET, Klitzman B, Secomb TW, Vinuya RZ, Dodge R, Brizel D, Gross JF: Perivascular oxygen tensions in a transplantable mammary tumor growing in a dorsal flap window chamber, Radiat Res 1992, 130:171-182

81.   Jiang BH, Semenza GL, Bauer C, Marti HH: Hypoxia-inducible factor 1 levels vary exponentially over a physiologically relevant range of O2 tension, Am J Physiol 1996, 271:C1172-1180

82.   Middeldorp J, Kamphuis W, Sluijs JA, Achoui D, Leenaars CH, Feenstra MG, van Tijn P, Fischer DF, Berkers C, Ovaa H, Quinlan RA, Hol EM: Intermediate filament transcription in astrocytes is repressed by proteasome inhibition, FASEB J 2009, 23:2710-2726

83.   Katsetos CD, Draberova E, Legido A, Dumontet C, Draber P: Tubulin targets in the pathobiology and therapy of glioblastoma multiforme. I. Class III beta-tubulin, J Cell Physiol 2009, 221:505-513

84.   Prestegarden L, Enger PO: Cancer stem cells in the central nervous system--a critical review, Cancer Res 2010, 70:8255-8258

85.   Soeda A, Park M, Lee D, Mintz A, Androutsellis-Theotokis A, McKay RD, Engh J, Iwama T, Kunisada T, Kassam AB, Pollack IF, Park DM: Hypoxia promotes expansion of the CD133-positive glioma stem cells through activation of HIF-1alpha, Oncogene 2009, 28:3949-3959

86.   Luna G, Lewis GP, Banna CD, Skalli O, Fisher SK: Expression profiles of nestin and synemin in reactive astrocytes and Muller cells following retinal injury: a comparison with glial fibrillar acidic protein and vimentin, Mol Vis 2010, 16:2511-2523

87.   Katsetos CD, Del Valle L, Geddes JF, Assimakopoulou M, Legido A, Boyd JC, Balin B, Parikh NA, Maraziotis T, de Chadarevian JP, Varakis JN, Matsas R, Spano A, Frankfurter A, Herman MM, Khalili K: Aberrant localization of the neuronal class III beta-tubulin in astrocytomas, Arch Pathol Lab Med 2001, 125:613-624

88.   Kolenda J, Jensen SS, Aaberg-Jessen C, Christensen K, Andersen C, Brunner N, Kristensen BW: Effects of hypoxia on expression of a panel of stem cell and chemoresistance markers in glioblastoma-derived spheroids, J Neurooncol 2011, 103:43-58

89.   Diserens AC, de Tribolet N, Martin-Achard A, Gaide AC, Schnegg JF, Carrel S: Characterization of an established human malignant glioma cell line: LN-18, Acta Neuropathol 1981, 53:21-28

90.   Bar EE, Lin A, Mahairaki V, Matsui W, Eberhart CG: Hypoxia increases the expression of stem-cell markers and promotes clonogenicity in glioblastoma neurospheres, Am J Pathol 2010, 177:1491-1502

91.   Galli R, Binda E, Orfanelli U, Cipelletti B, Gritti A, De Vitis S, Fiocco R, Foroni C, Dimeco F, Vescovi A: Isolation and characterization of tumorigenic, stem-like neural precursors from human glioblastoma, Cancer Res 2004, 64:7011-7021

92.   Said HM, Polat B, Staab A, Hagemann C, Stein S, Flentje M, Theobald M, Katzer A, Vordermark D: Rapid detection of the hypoxia-regulated CA-IX and NDRG1 gene expression in different glioblastoma cells in vitro, Oncol Rep 2008, 20:413-419

93.   Holmquist-Mengelbier L, Fredlund E, Lofstedt T, Noguera R, Navarro S, Nilsson H, Pietras A, Vallon-Christersson J, Borg A, Gradin K, Poellinger L, Pahlman S: Recruitment of HIF-1alpha and HIF-2alpha to common target genes is differentially regulated in

References

neuroblastoma: HIF-2alpha promotes an aggressive phenotype, Cancer Cell 2006, 10:413-423

94.   Kaluz S, Kaluzova M, Liao SY, Lerman M, Stanbridge EJ: Transcriptional control of the tumor- and hypoxia-marker carbonic anhydrase 9: A one transcription factor (HIF-1) show?, Biochim Biophys Acta 2009, 1795:162-172

95.   Qiang L, Yang Y, Ma YJ, Chen FH, Zhang LB, Liu W, Qi Q, Lu N, Tao L, Wang XT, You QD, Guo QL: Isolation and characterization of cancer stem like cells in human glioblastoma cell lines, Cancer Lett 2009, 279:13-21

96.   Wang J, Sakariassen PO, Tsinkalovsky O, Immervoll H, Boe SO, Svendsen A, Prestegarden L, Rosland G, Thorsen F, Stuhr L, Molven A, Bjerkvig R, Enger PO: CD133 negative glioma cells form tumors in nude rats and give rise to CD133 positive cells, Int J Cancer 2008, 122:761-768

97.   Veselska R, Kuglik P, Cejpek P, Svachova H, Neradil J, Loja T, Relichova J: Nestin expression in the cell lines derived from glioblastoma multiforme, BMC Cancer 2006, 6:32

98.   Gardner LB, Li Q, Park MS, Flanagan WM, Semenza GL, Dang CV: Hypoxia inhibits G1/S transition through regulation of p27 expression, J Biol Chem 2001, 276:7919-7926

99.   Goda N, Ryan HE, Khadivi B, McNulty W, Rickert RC, Johnson RS: Hypoxia-inducible factor 1alpha is essential for cell cycle arrest during hypoxia, Mol Cell Biol 2003, 23:359-369

100.   Khain E, Katakowski M, Hopkins S, Szalad A, Zheng X, Jiang F, Chopp M: Collective behavior of brain tumor cells: The role of hypoxia, Phys Rev E Stat Nonlin Soft Matter Phys 2011, 83:031920

101.   Grille SJ, Bellacosa A, Upson J, Klein-Szanto AJ, van Roy F, Lee-Kwon W, Donowitz M, Tsichlis PN, Larue L: The protein kinase Akt induces epithelial mesenchymal transition and promotes enhanced motility and invasiveness of squamous cell carcinoma lines, Cancer Res 2003, 63:2172-2178

102.   Zagzag D, Lukyanov Y, Lan L, Ali MA, Esencay M, Mendez O, Yee H, Voura EB, Newcomb EW: Hypoxia-inducible factor 1 and VEGF upregulate CXCR4 in glioblastoma: implications for angiogenesis and glioma cell invasion, Lab Invest 2006, 86:1221-1232